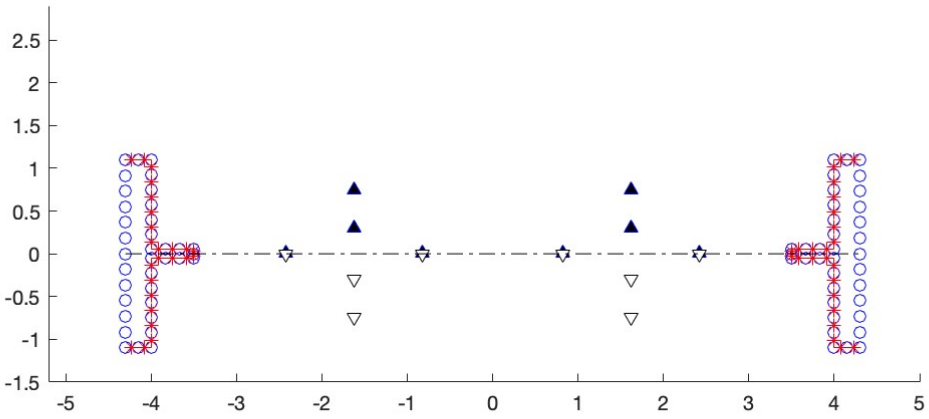

Noise Reduction Potential of Absorptive Low-Height Noise Screens and Trench-Like Segments

Estimating Insertion Loss from Urban Traffic Scenarios

Master's thesis in Applied Acoustics

ELLA STÅLHANDSKE
CHARLOTTE ÖSTERLUND

DEPARTMENT OF ARCHITECTURE AND CIVIL ENGINEERING
CHALMERS UNIVERSITY OF TECHNOLOGY
Gothenburg, Sweden 2025
www.chalmers.se

Master's thesis 2025

Noise Reduction Potential of Absorptive Low-Height Noise Screens and Trench-Like Segments

Estimating Insertion Loss from Urban Traffic Scenarios

ELLA STÅLHANDSKE
CHARLOTTE ÖSTERLUND

CHALMERS
UNIVERSITY OF TECHNOLOGY

Department of Architecture and Civil Engineering
Division of Applied Acoustics
Chalmers University of Technology
Gothenburg, Sweden 2025

Noise Reduction Potential of Absorptive Low-Height Noise Screens and Trench-Like Segments
Estimating Insertion Loss from Urban Traffic Scenarios
ELLA STÅLHANDSKE, CHARLOTTE ÖSTERLUND

Supervisor: Jens Forssén, Division of Applied Acoustics
Examiner: Jens Forssén, Division of Applied Acoustics

Master's Thesis 2025
Department of Architecture and Civil Engineering
Division of Applied Acoustics
Chalmers University of Technology
SE-412 96 Gothenburg
Telephone +46 31 772 1000

Cover: Overview of the segmentation of geometry and spatial arrangement of sound sources for Case 2, Situation (3), see section 4.7.

Typeset in LaTeX
Printed by Chalmers Reproservice
Gothenburg, Sweden 2025

Abstract

Urban planning is facing growing difficulties due to increasing traffic noise in the cities. Low-height noise screens (**LHNS**) could be considered to be implemented instead of the common tall noise screens as noise reducing devices (**NRD**). An investigation of implementing multiple absorptive LHNS combined with trench-like road segments, i.e. as effective NRD in urban area was conducted. Trench-like segments are defined as strips adjacent to the road surface filled with sound-absorbing ground materials. In order to evaluate the effect of multiple absorptive LHNS and trench-like segments, three traffic cases were defined and evaluated.

The absorptive LHNS, with a height of 1.1 meters, were tested for six types of absorbing materials and for two variations of trench-like segments. Two noise prediction tools; Boundary Element Method (**BEM**) combined with analytical calculations and a commercial noise mapping software SoundPLAN using the Nord2000 model, were applied to obtain the insertion loss in terms of A-weighted equivalent levels (**IL**) for the different cases. The IL was evaluated for two different heights, 1.5 and 4 meters, as well as for three distances, 7.5, 15 and 30 meters. One case was applied to a realistic urban scenario at Gibraltarvallen in SoundPLAN.

The results from both BEM and SoundPLAN show that absorptive LHNS materials, such as Vitrumit, mineral wool and Wood wool cement board, consistently provide higher IL than reflective hard screens across all traffic cases. Meanwhile, trench-like segments, regardless of tested ground materials, have little to no effect on the IL. For all three cases, removing the trench, enabling a narrower placement of the screens, was found to improve the performance of absorptive LHNS.

The BEM results show a highest IL of 14.6 dB at the 1.5 meter receiver height for one of the traffic cases, while SoundPLAN yields 7.5 dB for the same case. At the 4 meter receiver position, BEM shows a highest IL of 12.5 dB while SoundPLAN gives 10.6 dB for the same case. BEM consistently displays higher insertion loss than SoundPLAN across all cases, indicating that BEM predicts a stronger noise reduction effect. Insertion loss for maximum levels were also obtained for SoundPLAN, however since no clear trends were found, no further investigation was conducted.

The case applied at Gibraltarvallen consisting of two absorptive LHNS on either side of the road, showed an IL of 5–8 dB on the ground floor, 2–4 dB on the middle floors and, 0–1 dB on the top floors. Two LHNS showed an improvement of 1 dB compared to a single LHNS. The sound propagation in the area shows that placing multiple absorptive LHNS along the road reduces the A-weighted equivalent sound level by up to 10 dB.

Keywords: low-height noise screens, trench-like segments, insertion loss, Boundary Element Method, SoundPLAN, acoustics, noise reducing device.

AI transparency

In this thesis, artificial intelligence (AI) has been used as a supporting tool to check grammar, spelling, and sentence structure. It has also been used to create tables and figures in LaTeX format. Additionally, it has been used for general LaTeX formatting and supported code debugging.

Acknowledgements

We would like to express our appreciation to our supervisor and examiner, Jens Forssén. His guidance, support, and continuous presence have been incredibly valuable throughout this thesis. We are especially thankful for his willingness to share knowledge and provide insights essential for this thesis. We also truly appreciate his availability and quick responsiveness, even outside regular hour at times, been incredibly valuable to us.

Ella Stålhandske and Charlotte Österlund,
Gothenburg, June 2025

List of Acronyms

Below is the list of acronyms that have been used throughout this thesis listed in alphabetical order:

AADT	Annual average daily traffic
BEM	Boundary Element Method
dB	Decibel
IL	Insertion loss
L_{Aeq}	A-weighted Equivalent Continuous Sound Pressure Level
L_{AFmax}	A-weighted Maximum Sound Pressure Level
LHNS	Low-height noise screens
NRD	Noise reducing device
SPL	Sound pressure level
WWCB	Wood wool cement board

Nomenclature

Below is the nomenclature of indices, symbols, parameters, and variables that have been used throughout this thesis.

Indices

i	Index for vehicle type
j	Index for source type

Symbols

k_f	Width of lane [m]
L	LHNS
M	Central reservation
S	Soft top layer of LHNS [m]
v_f	Side shoulder [m]
v_l	Central shoulder [m]
v_m	Central hard shoulder [m]
v_r	Side hard shoulder [m]

Parameters

α	In Section 2.2 and 4.2.2, absorption coefficient [-]
	In Chapter 3, horizontal spatial frequency variable [rad/m]
	In Section 4.1.1, receiver angle [$\circ$]
$a_P(f)$	Propulsion coefficients [-]
$a_R(f)$	Tyre/road coefficients [-]
$b_P(f)$	Propulsion coefficients [-]

$b_R(f)$	Tyre/road coefficients [-]
β	Scaling factor [-]
c_0	Speed of sound in air [m/s]
C	Complex compressibility [-]
d	Thickness of porous material layer [m]
k_0	Wave number [rad/m]
k_c	Complex wave number [rad/m]
k_s	Structure factor in the medium [-]
L_p	Sound pressure level [dB]
$L_{p,d}$	Direct sound pressure level [dB]
$L_{p,tot}$	Total sound pressure level [dB]
$\Delta L_{p,airattenuation}$	Air attenuation loss per meter [dB/m]
$\Delta L_{p,i}$	Correction term [dB]
$N_{perhour}$	Number of vehicles per hour [-]
$N_{sourcelanes}$	Number of source lanes [-]
ω	Angular frequency [rad/s]
ϕ	Porosity [-]
p	Sound pressure [Pa]
$p_{n,i}$	Sound pressure at surface element i [Pa]
p_i	Vehicle type distribution [-]
r	Radial distance from source [m]
$\underline{r}$	Reflection coefficient [-]
r_i	Distance from surface element i to receiver [m]
$r_{direct,j}$	Direct distance from source to receiver [m]
$r_{image,j}$	Distance to receiver from image source [m]
R_p	Plane wave reflection coefficient [-]
ρ	Density [kg/m^3]
ρ_0	Density of air [kg/m^3]
σ	Flow resistivity [kNs/m^4]
ΔS	Area of surface element i [m^2]
θ_i	Incident angle [-]
θ_t	Transmission angle [-]
ϑ	Angle between the surface normal and the vector toward the field point [rad]
T	Tortuosity

v	Vehicle speed [km/h]
v_{ref}	Reference speed [km/h]
$v_{n,i}$	Normal particle velocity at surface element [m/s]
q_i	Volume flow rate of monopole
Q	Reflection coefficient [-]
$x_{receiver,j}$	Horizontal position of receiver [m]
$x_{source,j}$	Horizontal position of source [m]
y	Lateral distance along the road [m]
Δy	Offset used in spatial discretization [-]
$z_{receiver}$	Height of receiver [m]
z_{source}	Height of source [m]
Z_0	Characteristic acoustic impedance [Pa · s/m]
Z_c	Characteristic complex impedance of a porous material [Pa · s/m]
Z_s	Surface impedance [Pa · s/m]

Variables

f	Frequency [Hz]
$F(w)$	Boundary loss factor
IL	Insertion loss [dB]
IL_{max}	Maximum insertion loss [dB]
L_{Aeq}	A-weighted equivalent sound pressure level [dB(A)]
$L_{Aeq,24h,withoutscreen}$	A-weighted equivalent sound pressure level over 24 hours without screen [dB(A)]
$L_{Aeq,24h,withscreen}$	A-weighted equivalent sound pressure level over 24 hours with screen [dB(A)]
$L_{Aeq,withoutscreen}$	A-weighted equivalent sound pressure level without screen [dB(A)]
$L_{Aeq,withscreen}$	A-weighted equivalent sound pressure level with screen [dB(A)]
$L_{Amax,road,withoutscreen}$	A-weighted maximum sound pressure level without screen [dB(A)]
$L_{Amax,road,withscreen}$	A-weighted maximum sound pressure level with screen [dB(A)]
$L_{eq,i,j}$	Equivalent sound pressure level for vehicle type i and source type j [dB]
$L_{eq,i,sum,1}$	Equivalent sound pressure level for vehicle type i summed over source types j [dB]

$L_{eq,i,sum,2}$	Equivalent sound pressure level for vehicle type i summed over vehicle lanes [dB]
$L_{eq,i,j,sum}$	Equivalent sound pressure level for vehicle type i and source type j summed over road length [dB]
$L_{eq,withoutscreen}$	Equivalent sound pressure level without screen [dB]
$L_{eq,withscreen}$	Equivalent sound pressure level with screen [dB]
$L_{W,i,j}$	Sound power level for vehicle type i and source type j [dB]
$L_{WP}(f)$	Sound power level generated by the propulsion [dB]
$L_{WR}(f)$	Sound power level generated by the tyre/road interaction [dB]
$\Delta L_{W,i}$	Traffic flow correction to sound power level for vehicle type i [dB]
$\Delta L_{p,j,hardground}$	Ground reflection correction for source type j [dB]
$\Delta L_{p,transfer,j,FREE}$	Transfer single source line for source type j for free field [dB]
$\Delta L_{p,transfer,j,REF}$	Transfer single source line for source type j for reference [dB]
$\omega_{eq,i,j}$	Equivalent sound energy for vehicle type i and source type j
$p(r_{mic}, \omega)$	Sound pressure at microphone in free-field [Pa]
$p(x, z, \sqrt{k^2(\nu) - \alpha^2})$	2D sound pressure field
$P(x, y, z, k(\nu))$	3D sound pressure field

Contents

List of Figures

List of Tables

1
Introduction

1.1 Background

Modern society faces an increasing problem with traffic noise in urban areas. Noise affect the majority of people in Sweden and traffic is the dominating source of it. The noise could have bad health effects, both short-term and long-term, such as sleep difficulties and increased risk of cardiovascular diseases [5]. It is therefore important to try to reduce traffic noise to get a better environment and management of it is a key aspect of urban planning. Noise reducing devices (**NRD**) have therefore become important in controlling and combating traffic noise. Today, one of the most common used NRD is tall noise screens due to their effectiveness and predictability. However, they are not always suitable due to their large size, which significantly alters the landscape and can have an unpleasant impact on the urban environment. In these cases, low-height noise screens (**LHNS**) may be more suitable to preserve the existing urban environment while combating traffic noise. However, because of their limited height, their ability to block sound might not be sufficient and requires the LHNS to rely on geometrical designs and dampeners to achieve sound reduction and diffraction.

With the goal of evaluating the effectiveness and feasibility of low barriers, Chalmers University of Technology wants to investigate how different geometric configurations, in combination with absorbing materials, can improve traffic noise reduction in an urban setting. This is done in an effort to enable wider usage of NRD. Previous work by C. Burgos and L. Wåssén showed that LHNS reduces traffic noise but found the reduction insufficient, in many cases, to meet Swedish regulations [6]. This thesis can be seen as an extension of their work, exploring new geometrical configurations by using multiple LHNS combined with various absorbing materials to investigate whether further noise reduction can be achieved. Furthermore, their work regarding the implementation of LHNS in relation to the Swedish regulations is highly relevant for this thesis, as the use of multiple LHNS introduces additional challenges in meeting these regulations.

In the past, the available methods used to estimate noise reduction with LHNS have been limited. This issue has been addressed in previous work by M. Hildén [7] and P. Eriksson [8], who worked on developing a Boundary Element Method (**BEM**) model previously created by B. van der Aa [9] to improve the estimation of LHNS for rail traffic. This thesis will additionally expand their work to include more extensive geometric configurations, allowing multiple and absorbing LHNS with application for road traffic.

1.2 Purpose/Aim

The aim of this thesis is to investigate the possibility of introducing LHNS at multiple edges of lanes, together with trench-like road segments to effectively reduce traffic noise. Additionally, the study aims to develop design proposals that optimize both material properties and geometric configurations to maximize noise attenuation while ensuring feasibility for urban planning. By doing so, we evaluate whether LHNS at multiple edges of lanes can be effectively utilized as an NRD, potentially enabling a wider application of LHNS in urban planning. For this investigation, two methods are used, BEM and the commercial noise mapping software SoundPLAN. Using both methods allow for a comparative analysis of results and enabling cross-validation of observed trends.

c

1.3 Scope

A BEM model will not be created due to previous work [7][8][9]. Instead, it will be modified and expanded to make it applicable to road traffic and aligned with the geometric requirements of this thesis. Furthermore, the thesis will not include describing the function, practical limitations and construction of LHNS due to previous work [6]. Additionally, when computing for traffic noise, the numerical modelling of BEM will have an upper frequency limitation of 5000 Hz, a standard frequency range when evaluating traffic noise [10]. Since the thesis focuses on Swedish regulations, limitations in geometry in BEM and in the commercial noise mapping software SoundPLAN will be considered. The designing of roads will not consider how to solve safe zones around the roads. If the LHNS are within the zone it is assumed that the barriers meet the safety requirements. Economic aspects will not be taken into consideration when creating the design proposals.

Within these limitations, the thesis will attempt to answer following central questions:

- What levels of insertion loss can be achieved through absorptive low height noise screens in combination with trench-like segments, and are these reductions acoustically and perceptually significant?
- What is the most optimized design proposal tested from an acoustic perspective?
- How well do our numerical calculations with BEM correspond to the simulations performed in SoundPLAN using the Nord2000 method? To what extent do these simulations reflect what would be expected in a real case scenario?

1.4 Thesis structure

The thesis will be divided into five main chapters. Chapters 2 and 3 provide an overview of key concepts and methods important for understanding the study. These

chapters contribute to a deeper knowledge of the methods that will be used to address the central questions of the thesis. In chapter 4, implementation of numerical modelling of BEM for different design proposals will be done. The implementation considers geometry and materials as well as information from the theory chapters. The chapter also includes further implementation of the design proposal in SoundPLAN. In chapter 5, the results from BEM and SoundPLAN will be presented to later be compared and discussed in chapter 6. Chapter 6 will also discuss limitations, uncertainties and potential areas where the topic can be expand for future work.

1.5 Division of work

The work has been carried out together for all parts, except for the written formulation of the report. All calculations, simulations, analysis and evaluation has been a joint effort and equally contributed to.

2
Theory

This chapter provides an overview of key concepts and principles important for understanding and applying the methods used in this thesis. It also includes the concept of traffic noise modelling and a summary of Swedish traffic regulations to consider.

2.1 Physical Principles

Sound waves in gas or fluid
Sound is a wave phenomenon in which energy is transmitted through a medium by vibration and pressure fluctuations [11]. When a source generates sound, it creates wave motion in the surrounding gas or fluid, this motion is known as sound waves. These waves are longitudinal waves that oscillates in the direction of the wave propagation. The direction of the propagating wave is determined by the surrounding fluid, its boundaries and the geometrical and vibrational properties of the radiating mechanical system. The period of distance until the wave repeats it self is called wavelength and is dependent on both the frequencies of oscillation and speed of sound in the medium of which the wave propagates through [1].

Plane waves
The simplest form of wave propagation is the plane wave. It describes a sound wave where the velocity of the particles and the pressure of the sound depend only on one single spatial coordinate. This means that at any given moment, these quantities remain constant across planes perpendicular to that coordinate. Furthermore, the plane wave propagates perpendicular to these planes, maintaining its sound pressure amplitude over distance as long as no effects of losses are present. The plane wave is important in acoustics, as it can be used to express more complex waveforms in an convenient way [12].

Spherical waves
A more complicated, but often more realistic wave propagation, is the spherical wave. This type of wave motion is generated by a sphere whose surface pulsates consistently, creating sound waves that propagate in all directions outwards into free space, creating spherical wave fronts. For an ideal sphere the sound field is spherically symmetric, meaning that the sound pressure is the same in all directions at any distances from the source. The sphere is often refereed to as a point source. The sound pressure amplitude of a point source decreases as the radial distance, r, increases [11].

Impedance
Ratios between different sound field quantities often play an important role in describing and solving problems in acoustics. The ratio between two independent quantities, called impedance, is a significant ratio and a central concept in acoustics. Impedance is often denoted as Z and is a frequency-dependent quantity. It is also a complex quantity consisting of both a real and an imaginary part, commonly expressed as magnitude and phase [1]. There are a number of different impedance used in acoustics and various other fields, but in this thesis, the primary focus is on characteristic impedance. The characteristic impedance is defined as the ratio of the sound pressure to particle velocity for an infinite plane wave, commonly represented as Z_0. It is equal to the product of the mediums density and speed of sound, $Z_0 = \rho * c$, if one assumes no propagating losses in the medium [1][13].

2.2 Sound propagation outdoors

Outdoor sound sources, such as vehicles, trains, and machines, generate waves propagating through air but can also cause structural waves. These structural waves refer to vibrations propagating through solids and are often referred to as structure-borne sound. Unlike gases, that primarily reacts to changes in pressure, solids also resists deformation causing both normal and shear forces. Structure-borne sound is often present in structures, such as buildings, and can cause sound to be radiated as airborne sound [14]. The airborne sound radiation from structure-borne sound is often significant inside structures but less important in the context of this thesis, which focus on traffic noise in the outdoor environment.

Reflection and transmission
Sound waves propagating outdoors between a sound source and a receiver have one direct path and multiple reflected paths, assuming no object obstructs the propagation except the ground. The direct sound wave travels straight from the source to the receiver, while the reflected waves interact with the ground before reaching the receiver. Depending on the reflecting surface, the amplitude and phase of the reflected waves changes before reaching the receiver. This often results in interference between the direct and reflected sound wave due to phase differences [15]. The change in phase and amplitude is the results of variations in the boundary between two media or changes of characteristic impedance. When a sound wave encounters such a boundary or impedance change, it splits into two parts. One part of the incident wave's power may be reflected, while the remaining power is transmitted into the new media or impedance region. The power of the incident wave is divided between the reflected and transmitted sound wave [1]. Wave propagation outdoors occurs in air. Assuming homogeneous conditions (constant temperature and no wind) the sound traveling through the air will remain unaffected. The reflected and transmitted waves will therefore be a result from changes in characteristic impedance due to the ground. This phenomenon is often referred to as ground effect and in illustrated in Figure 2.1.

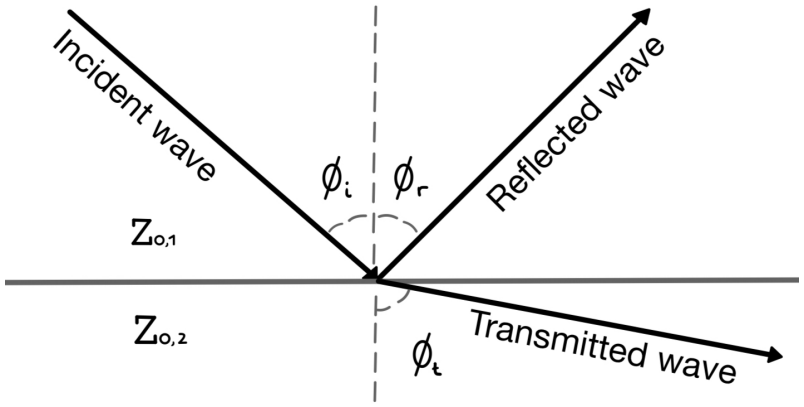

Figure 2.1: Own illustration inspired by [1], illustrating wave reflection and transmission at a boundary between two materials with different acoustic impedance. The incident wave is partially transmitted and partially reflected.

The ratio between reflected and transmitted power is determined by three factors: the change of characteristic impedance between the two medium, $Z_{0,1}$ and $Z_{0,2}$, the incident angle, ϕ_i and the transmission angle, ϕ_t. At normal incidence, the reflection coefficient, which describes the ratio between the reflected and incident sound pressures, is given by Equation 2.1. When energy from the transmitted wave is absorbed by the material, the sound absorption coefficient is given by Equation 2.2.

$$\underline{r} = \frac{\underline{\hat{p}}_r}{\underline{\hat{p}}_i} = \frac{\underline{Z}_2 - \underline{Z}_1}{\underline{Z}_2 + \underline{Z}_1} \tag{2.1}$$

$$\alpha = 1 - |\underline{r}|^2 \tag{2.2}$$

When sound propagation occurs at an boundary where the sound wave has an non-normal angle of incidence, the direction of propagation is determined by Snell's law. In this case the reflection coefficient can be formulated as seen in Equation 2.3 [1].

$$\underline{r} = \frac{Z_{0,2}\cos(\phi_i) - Z_{0,1}\cos(\phi_t)}{Z_{0,2}\cos(\phi_i) + Z_{0,1}\cos(\phi_t)} \tag{2.3}$$

This reflection coefficient is determined for plane waves and not suitable for wave propagation outdoors. In an outdoor environment one often assume the sound propagation to be spherical. To explain the ratio of transmitted and reflected waves outdoors, the spherical reflection factor, Q, is used. The spherical reflection factor can be expressed by modifying the reflection coefficient for plane waves with a boundary loss factor, expressed in Equation 2.4 [16].

$$Q = R_p + (1 - R_p)F(w) \tag{2.4}$$

Diffraction

Diffraction around a barrier could be explained through Huygens' principle which states that every point on a wavefront acts as a new sound source after passing a diffracting edge. These point sources radiate sound energy even into the shadow zone. The direct sound path between a source and a receiver will be blocked if a barrier is introduced between them. Instead of going in straight lines, the sound waves could change the direction and bend around the edges of the barrier. This bending is called diffraction. The amount of diffraction depends on the frequency of the sound wave and the size of the obstacle. Low frequency sounds will diffract easier, while if it is more high frequency sounds it will diffract less. This means that barriers effectiveness becomes frequency dependent due to diffraction, making the screens more effective at higher frequencies than lower frequencies [12], [17].

2.3 Outdoor impedance models

When assessing outdoor noise levels, it is important to analyse the ground effect in sound propagation. Ground effects occur due to interference between the direct sound and reflected sound when the source and receiver are close to the ground [16]. The ground effect depends on the type of ground in the surrounding area. To estimate ground effect, outdoor ground impedance models have been developed. Among the various impedance models, the Delany and Bazley impedance model is widely used for outdoor sound prediction and is used in Nord2000.

The Delany-Bazley model is a simplified approach that uses only one parameter, effective flow resistivity, to model ground effects [18]. Flow resistivity is a measure of how easily air can flow in and out of the ground [16]. The model assumes a locally reacting semi-infinite homogeneous material, where "locally reacting" means that the interaction between the air and the ground does not depend on the angle of incidence of the incoming wave [16], [18].

The characteristic complex impedance Z_c can be calculated using Equation 2.5 based on Delany and Bazley impedance model, where σ is flow resistivity and f represents the centre frequencies of third-octave bands ranging from 25 Hz to 10 kHz according to Nord2000 [19]. Flow resistivity values are defined in Nord2000 for different ground surfaces. Equation 2.6 is the corresponding complex wave number.

$$Z_c = 1 + 0.0571\left(\frac{\rho_0 \cdot 2\pi f}{2\pi\sigma}\right)^{-0.754} + i0.087\left(\frac{\rho_0 \cdot 2\pi f}{2\pi\sigma}\right)^{-0.732} \tag{2.5}$$

$$k_c = k_0\left(1 + 0.0978\left(\frac{\rho_0 2\pi f}{2\pi\sigma}\right)^{-0.7} + i0.189\left(\frac{\rho_0 2\pi f}{2\pi\sigma}\right)^{-0.595}\right) \tag{2.6}$$

If one assumes that the porous layer is placed on a rigidly backed layer, the surface impedance can be calculated with the help of the porous layer's thickness, see Equation 2.7 [20].

$$Z_s = Z_c \coth(-ik_c d) \tag{2.7}$$

The Delany and Bazley model does not work well in some cases of soft ground types, such as porous asphalt, for estimating ground effect in low frequencies [20]. This

results in that the model is for example sufficient when calculating impedance of a barrier consisting of mineral wool but not fitted for soft ground. To try to improve this aspect, modifications of the Delany and Bazley model were made and a new model called Miki developed [21], [22]. The characteristic complex impedance Z_c and the corresponding complex wave number k_c can be calculated using Equation 2.8 and 2.9. However, when the Miki model was reviewed and compared to Delany and Bazley, it was found that the model had the same problems at low frequencies [22]. It results in that the model is, as the previous model, a good model to use for porous materials such as mineral wool but not for soft ground.

$$Z_c = 1 + 5.5\left(\frac{1000f}{\sigma}\right)^{-0.632} + i8.43\left(\frac{1000f}{\sigma}\right)^{-0.632} \tag{2.8}$$

$$k_c = k_0\left[1 + 7.81\left(\frac{1000f}{\sigma}\right)^{-0.618} + i11.41\left(\frac{1000f}{\sigma}\right)^{-0.618}\right] \tag{2.9}$$

Zwikker and Kosten phenomenological model is another impedance model which can be used and is based on three parameters: flow resistivity σ, porosity ϕ and structure factor k_s. The variables used in the Zwikker and Kosten model for the characteristic complex impedance and complex wave number are defined in Equations 2.10–2.11 [23].

$$Z_c = \sqrt{\frac{i\,\sigma}{\rho_0\,\omega\,\phi} + \frac{k_s}{\phi^2}} \tag{2.10}$$

$$k_c = k_0\sqrt{\frac{i\,\sigma\,\phi}{\rho_0\,\omega} + k_s} \tag{2.11}$$

To calculate the impedance for soft ground, an additional impedance models, the slit-pore model is introduced. The slit-pore model is based on two parameters: flow resistivity and porosity. The characteristic complex impedance and the complex wavenumber for the slit-pore model are given in Equations 2.12–2.13 where T is tortuosity and C is the complex compressibility [20].

$$Z_c = (\rho_0 \cdot c_0)^{-1} \cdot \sqrt{\frac{T}{\phi^2} \cdot \frac{\rho}{C}} \tag{2.12}$$

$$k_c = \omega \cdot \sqrt{T \cdot \rho \cdot C} \tag{2.13}$$

Other impedance models are based on multiple parameters compared to the models mentioned earlier. These models can become too complex to use due to factors such as characteristic lengths and pore shape factors being unknown for the ground, making them unsuitable for outdoor ground surfaces [20].

2.4 Road traffic

Key metrics for traffic noise
The equivalent noise level, $\mathbf{L_{Aeq}}$ is used to describe the average sound pressure level, over a certain duration of time, A-weighted. LAeq,24 h is often used to describe long-term noise exposure from traffic during a 24-hour period.

Maximum noise level, $\mathbf{L_{AFmax}}$ displays the maximum sound pressure level over a certain time with fast time weighting and A-weighting. It is used to identify short peaks in the sound pressure[24].

Nord2000
The National Noise Coordination (*In Swedish: Nationella bullersamordningen*) recommends using Nord2000 to calculate road and rail traffic noise to achieve greater accuracy and improved calculation results compared to the previously recommended standards Nord96-road and Nord96-rail. Nord2000 is recommended for application to road traffic starting June 1, 2024, and to rail traffic starting January 1, 2025 [25].

Nord2000 is able to calculate sound pressure levels for traffic noise in third-octave bands between centre frequencies of 25 Hz and 10 kHz. The new prediction method can, in theory, deal with multiple noise barriers but, in practice, it is only two that can be considered due to practical limitations. Vehicles are divided into three main categories; light, medium and heavy, each with different subcategories. The prediction method can calculate for complex terrains and different weather conditions. The weather conditions can be divided in three groups; neutral, actual condition and yearly average.

There are eight main categories for road surfaces and seven main groups for ground surfaces. The categories for road surfaces varies from dense asphalt and porous asphalt to paving stones and cement block pavement. The categories for ground surfaces ranges from very soft, such as snow or moss-like, to hard, like concrete and dense asphalt. Even though, ground surfaces is divided into seven classes, it generally is grouped as soft or hard when mapping the noise. The ground surfaces have representative flow resistivities which is used in Nord2000 [26], [27].

Nord2000 introduces the concept of so-called Fresnel zones. These Fresnel-zones can be used when modelling the sound propagation over mixed grounds. The ground types found within a Fresnel-zone are calculated separately before determining the total ground effect using a weighted average. The calculation of the total ground effect depends on how much of the Fresnel zone is covered by each ground type. By using Fresnel-zones, Nord2000 improves the accuracy of modelling sound propagation, especially over mixed ground types [27].

Vehicles as noise sources
A road vehicle has multiple sources that generate noise; the main ones are the engine, the exhaust, the transmission, the tyres and the car body. These sources can be categorized into three main categories, propulsion noise, tyre/road noise and aerodynamic noise. The propulsion noise consists of the sound emitted from the engine, transmission and exhaust of a vehicle. Tyre/road noise comes from the interaction between the tyre and the road which causes sound to radiate. Tyre/road noise is the dominating noise source under normal circumstances above 800 Hz.

The sound is also directional, radiating more in the forward direction in the higher frequencies. The last category is the aerodynamic noise, occurring along the vehicles body. Aerodynamic noise is speed dependent, and can often be neglected at low speeds but important at grater speeds [26].

The recommended source model, for vehicles in the Nordic countries, is based on the Harmonoise source model and modified to be applicable to Nord2000. For this source model the vehicles are divided into three main categories, light, medium and heavy vehicles. There are further categories for medium and heavy vehicles which categories the vehicles further depending on type and number of axes. Simply put, medium vehicles have two axes while heavy vehicles have at least three axes. Each vehicle is also divided into different sound sources, at specific heights. Each vehicle is usually simplified to have two sound sources, tyre/road noise and propulsion noise. The two sound sources are represented as point sources that radiate spherical waves. These sources are placed at different heights in relation to the origin of the noise and vehicle type, these heights can be found in Table 2.1. In Nord2000, all sources is located on the side of the vehicle nearest to the receiver at a distance of 1 meter from the vehicle centre line [28].

Table 2.1: Source locations for different vehicle categories

Vehicle type	Source	Height (m)
Light	Tyre/road	0.01
	Propulsion	0.30
Medium	Tyre/road	0.01
	Propulsion	0.75
Heavy	Tyre/road	0.01
	Propulsion noise	0.75

The sound power level for vehicles, in accordance with Nord2000, is determined by adding the sound power generated by the tyre/road interaction, Equation 2.14, as well as the vehicles propulsion, Equation 2.15. The sound power levels are determined by a set of coefficients, a_R, b_R, a_P, b_P developed in the Harmonise Project as well as a reference speed of 70 km/h, v_{ref} and the real speed v. It was later established that these coefficients where not suitable to be used in Nord2000 for the Nordic countries and a revision was made. The revised coefficient where established to ensure better accuracy and regional specific noise predictions and where created to fit the Danish Nord2000. The revised coefficient are referred to as DK Nord2005. The sound power coefficients in DK Nord2005 are presented in Appendix A[3]. The coefficients are applicable direly on danish roads. In Nord2005 corrections for Swedish, Norwegian and Finnish roads are also presented for the tyre/road coefficients, a_R, [3]. These corrections where later discovered to overestimate noise emission when compared to new measurements of noise emissions from vehicles in Sweden. It was also discovered that the propulsion noise was overestimated for Nord2000 in Sweden, which new corrections for the propulsion coefficient a_P was suggested. These corrections are presented in Appendix A[4].

$$L_{WR}(f) = a_R(f) + b_R(f) lg \frac{v}{v_{ref}} \tag{2.14}$$

$$L_{WP}(f) = a_P(f) + b_P(f) \frac{v - v_{ref}}{v_{ref}} \tag{2.15}$$

Design of an absorbent LHNS for road implementation
Absorbent LHNS have sound absorbing materials on the side facing the road to reduce reflections between vehicles and the screen. Compared to a standard high barrier, LHNS rely more on sound absorption within the barrier and its surface materials, as well as reflections between the road surface and vehicles, to dissipate acoustic energy. The distance between the noise source and the barrier is relatively short. The soft ground strips between the vehicle and the barriers, see Figure 2.2, are an additional feature designed to help minimize reflections using the ground effect. Absorptive material can also be implemented on the top of the screen to further reduce reflections of sound waves.

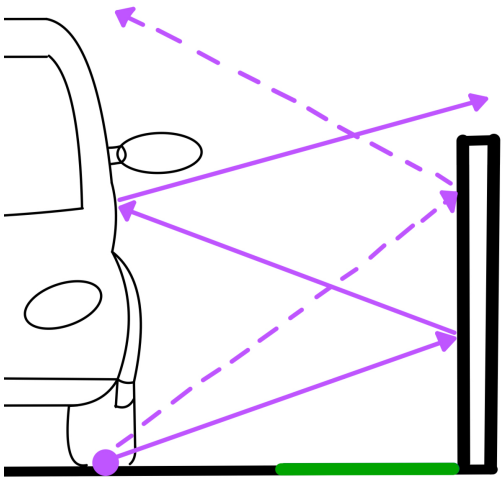

Figure 2.2: Example illustration of a road setup for evaluating the impact of LHNS and soft ground regarding traffic noise reduction

Geometrical restraints
There are many rules and regulations that must be followed when designing roads and depending on what kind of road it is, the regulations are different. These regulations are generally based on guidelines from Trafikverket, the Swedish transport administration, but in some cases, local traffic regulations may complement them. This chapter presents the regulations that apply to a through street with one lane in each direction with a speed limit of 40 km/h, as well as a divided highway with two lanes in each direction with a speed limit of 80 km/h.

A through street with one lane in each direction, with a speed limit of 40 km/h, follows Trafikverket's standards but local regulations also apply if the road is located in Gothenburg. *Göteborgs Stad*, the municipality of Gothenburg, has a technical

handbook including local regulations for road traffic. For example, it includes geometric dimensioning guidelines for through streets with 40 km/h speed limit roads may have two to four lanes. The recommended road width, including side shoulders, is 7.0 meter for a two-lane road. When implementing a LHNS for this type of road, there must be a unobstructed width of at least 0.5 meters between the road and any obstacle higher than 0.2 meters [29].

According to national regulations the side of road, also called shoulder v, must include a side hard shoulder v_r made of asphalt which must be at least 0.25 meter wide and connected to the lane on each side of the road. This shoulder can be counted toward the unobstructed width between the LHNS and the lane. The remainder of the shoulder, known as side shoulder v_f, may consist of soft material such as gravel or grass, or asphalt [30]. If a central reservation is added, consisting for example of a barrier and a grass strip, there must also be a minimum unobstructed width of 0.5 meters from the lane to the LHNS. A central hard shoulder v_m of at least 0.25 meter should then be included and connected to the lane. The remaining part of that shoulder, called central shoulder v_l, can be made of different materials, just like v_f. If there is no central reservation, the lanes are adjacent and no shoulder is needed between them, resulting in a narrower road. The geometrical requirements for a through street with one lane in each direction, speed limit 40 km/h, are summarized in Table 2.2.

Table 2.2: Geometrical dimensions for a through street with one lane in each direction, speed limit 40 km/h, based on Göteborgs Stad and Trafikverket's regulations.

Road feature	**Dimension**
Recommended total road width (2 lanes + shoulders)	7.0 m
Unobstructed path to LHNS	$\geq$ 0.5 m
Side hard shoulder (v_r)	$\geq$ 0.25 m
Side soft shoulder (v_f)	Optional (no fixed dimension)
Central hard shoulder (v_m)	$\geq$ 0.25 m

When designing a divided highway with a speed limit of 80 km/h according to Trafikverket, the lane width, designated as k_f, should be between 3.25 and 4.0 meters. For new roads, the minimum required width is 3.5 meters. There must a central reservation between opposing traffic lanes. This reservation, designated as M, must be at least 0.3 meters wide. The central hard shoulder v_m must be at least 0.6 meters wide. Trafikverket also states that the side hard shoulder v_r must be at least the width of the edge line plus 0.05 meters, which results in a minimum width of 0.35 meters. The same requirement for unobstructed width between the road and an obstacle applies here, with a v_r of 0.35 meters, the minimum width for v_f is then 0.15 meters [30]. The geometrical requirements for a divided highway with 80 km/h speed limit, are summarized in Table 2.3.

Table 2.3: Geometrical dimensions for a divided highway with 80 km/h speed limit, based on Trafikverket's regulations.

Road Feature	**Dimension**
Lane width (k_f)	3.25–4.00 m (min. 3.5 m for new roads)
Central reservation (M)	$\geq$ 0.3 m
Central hard shoulder (v_m)	$\geq$ 0.6 m
Side hard shoulder (v_r)	$\geq$ 0.35 m (edge line + 0.05 m)
Side soft shoulder (v_f)	$\geq$ 0.15 m (to reach 0.5 m unobstructed width)
Unobstructed path to LHNS	$\geq$ 0.5 m

The LHNS height should also needs to be considered, especially in urban areas where pedestrians and bicycle traffic is more common than on highways. For safety reasons, the LHNS cannot be too high. The eye level when driving a passenger car is approximately 1.1 meters, which is the lowest height among all vehicle types. Therefore, the LHNS should be considered to be dimensioned after this height [31].

3

Barrier modelling in BEM

To evaluate LHNS one method that previously work has found effective has been numerical calculations with BEM. BEM is a numerical computational method that can be used when solving radiation problems. It can also be used to estimate how well noise barriers reduce traffic noise [10]. Basic concepts relevant to BEM is presented here. For further reading, see references [32] and [10].

Rayleigh integral

BEM can be implemented for the Rayleigh integral. The Rayleigh integral can be used for certain geometries, such as plate in baffled structure, or to estimate total radiated sound power. The integral is an analytical approach in which a structure is divided into surfaces. These surfaces are discretized into N elements, where each elements is replaced by a monopole placed at its center, see Figure 3.1. The monopoles act as sound sources to calculate the sound pressure at microphone in free-field, see Equation 3.1. The q_i is volume flow rate of the monopoles and r_i the distance from monopole to receiver [2].

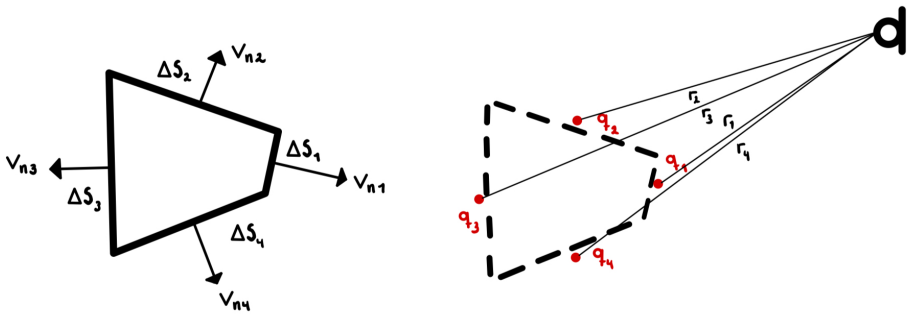

Figure 3.1: Own illustration inspired by [2], illustrating surfaces replaced by monopole sources located at the centre of each element.

$$p(r_{\text{mic}}, \omega) = j\omega\rho \sum_{i=1}^{N} \frac{q_i}{4\pi r_i} e^{-jk_0 r_i} \tag{3.1}$$

Kirchhoff-Helmholtz integral

For some cases it can be sufficient to use the Rayleigh integral in an effort to estimate sound radiation in BEM. However, the Rayleigh integral is only valid for sound radiation from a plane surface, baffled by a rigid wall. The Rayleigh integral can therefore only process cases where the source is mounted in an rigid baffle. To implement more complex geometries, such as LHNS, one can not use the Rayleigh integral since it does not account for scattering. For numerical calculations in BEM, for more complex geometries, the Kirchhoff-Helmholtz integral is better suited. To account for scattering on the "body" a dipole source is introduced to each monopole source, see Figure 3.2 and Equation 3.2. A monopole is only capable of changing amplitude, while a dipole can change amplitude and direction, thus enabling scattering to be accounted for [2].

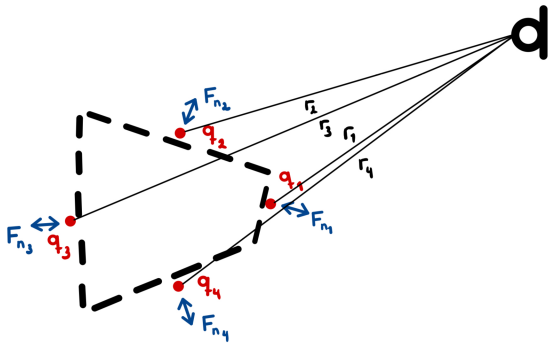

Figure 3.2: Own illustration inspired by [2], illustrating surfaces replaced by monopoles and dipoles located at the centre of each element.

$$p(r_{\text{mic}},\omega) = j\omega\rho \sum_{i=1}^{N} \frac{v_{n,i}\Delta S}{4\pi r_i} e^{-jk_0 r_i} + \sum_{i=1}^{N} p_{n,i}\Delta S \frac{\cos\vartheta_i}{4\pi r_i}\left(\frac{1}{r_i} + jk_0\right) e^{-jk_0 r_i} \tag{3.2}$$

2.5D Geometry

By solving the Kirchhoff-Helmholtz integral the pressure for a 2D geometry can be established. However, according to Nord2000, when sources cannot be expressed as one single point source, it has to be approximated by a number of incoherent point sources [19]. In the 2D approximation, the sources are assumed to be homogeneous extensions of point sources, which inaccurately represents the situation with road traffic addressed in this thesis. To extend to incoherent point sources without requiring a 3D model, which requires a lot of computational time, a 2.5D Fourier transform is applied. This technique reconstruct the 3D pressure field from a 2D pressure, see Equation 3.3 [32], [10].

$$P(x,y,z,k(\nu)) = \frac{1}{2\pi}\int_{-\infty}^{+\infty} e^{i\alpha y} p\left(x,z,\sqrt{k^2(\nu)-\alpha^2}\right) d\alpha \tag{3.3}$$

where P is the 3D sound pressure field at position (x,y,z) and wavenumber k(ν), p is the 2D pressure field in the xz-plane for wavenumber $\sqrt{k^2(\nu)-\alpha^2}$ arising from a Fourier transform in the y-coordinate.

4
Methods

In order to estimate the effects of trench-like segments, i.e. strips of acoustically soft ground adjacent to the road, and multiple LHNS, two different methods has been used; BEM combined with analytical calculations and simulations in the commercial noise mapping software SoundPLAN. BEM is a well documented numerical method that has been adopted and implemented to use for calculating IL for LHNS [33]. SoundPLAN is a widely used software in urban planning. SoundPLAN uses Nord2000, which is commonly applied in noise assessments, enabling direct comparison with results from BEM. The software is relevant not only from a scientific aspect but also for evaluating the applicability of LHNS in real world scenarios.

Three traffic cases, based on common urban scenarios was defined. Each case is evaluated in three situations, (1) without LHNS or trench-like segments, (2) with multiple LHNS but no trench-like segments and (3) with both LHNS and trench-like segments. Situation (1) was the reference situation without any noise reducing devices. All three cases, traffic situations, was evaluated with BEM (combined with analytical solutions) and by noise mapping software. The following chapter present the approached used to carry out the analysis of LHNS and trench-like segments for road traffic. The geometry of the evaluated traffic scenarios are presented below since they are applied for both methods. The implementation is then further explained in Section 4.1.3 and 4.2.1.

Geometry
To estimate the effects of trench-like segments and multiple LHNS three different cases has been evaluated. These different cases has been constructed to simulate three common traffic situations to evaluate whether trench-like segments and multiple LHNS are beneficial in real urban situations. The geometric structure of each case has therefore been designed to abide the local and national Swedish regulations. To evaluate the effects each case was evaluated in three situation: first, without LHNS and trench-like segments; secondly, with multiple LHNS but no trench-like segments; and finally, with both multiple LHNS and trench-like segments. The first situation, which excludes both LHNS and trench-like segments, was not treated using BEM due to its lower complexity and to reduce computational load. This situation was evaluated analytically, as described in section 4.1.6.

In this thesis, the implementation of absorptive LHNS also includes a soft top defined as an absorptive layer on top of the LHNS. This section provides a detailed description of all three cases and their geometrical configurations, based on local and national Swedish regulations. The geometrical constraints are not included in this section and can instead be found in Section 2.4. In order to comply with the

Swedish regulations while enabling the implementation of LHNS, the LHNS will be positioned within the designated safety zones but outside the obstacle-free zone. The LHNS are therefore assumed to be design to meet the requirements for objects inside the safety zone. To assess the acoustic performance of the LHNS, while maintaining computational efficiency, all three cases was based on a geometry where the height of the road surface and the surface behind the LHNS is defined as zero. These surfaces are treated as acoustically hard, and by defining their height as zero, computational time in BEM is significantly reduced.

Case 1: Urban two-lane road with noise barriers separating traffic directions and along the sides.
The first case was based on a two-lane road, one lane per direction, often occurring in urban cities. For these roads a vehicle speed of 40 km/h was estimated. Case 1 was evaluated in three different situations:

- Situation (1): Reference situation. No LHNS or trench-like segments are included.
- Situation (2): Three LHNS are included, two placed on either side of the road and one positioned between the lanes. No trench-like segments are included.
- Situation (3): Three LHNS are included, two placed on either side of the road and one positioned between the lanes. In this situation trench-like segments are added in front of each roadside LHNS as well as on both sides of the LHNS positioned between the lines.

Case 1 is simply illustrated in Figure 4.1 where the geometry consists of multiple different segments, each explained from Table 4.1. When implementing this geometry in BEM, it was simplified to include only a single vehicle and its adjacent LHNS to reduce computational time.

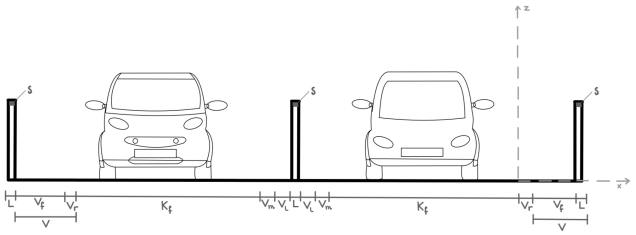

Figure 4.1: Sketch of Case 1 geometry: two-lane road, 40 km/h speed limit.

Table 4.1: Road segments Case 1.

		Width (m)			Height (m)		
		Situation			Situation		
Road segment	**Label**	**1**	**2**	**3**	**1**	**2**	**3**
LHNS	L	0.3	0.3	0.3	0	1.1	1.1
Soft top	S	0.3	0.3	0.3	0.05	0.05	0.05
Side shoulder	v_f	0.25	0.25	0.5	0	0	0.05
Side hard shoulder	v_r	0.25	0.25	0.25	0	0	0
Lane	k_f	3.25	3.25	3.25	0	0	0
Central hard shoulder	v_m	0	0.25	0.25	0	0	0
Central shoulder	v_l	0	0.25	0.5	0	0	0.05

Case 2: Urban two-lane road with side noise barriers.
The second case was based on the same type of road as case 1, a two-lane road with vehicle speed of 40 km/h. This case includes two LHNS compared to three, which could prove to be more cost effective and more feasible to implement in existing infrastructure. This case was also evaluated in three situations:

- Situation (1): Reference situation. No LHNS or trench-like segments are included.
- Situation (2): Two LHNS are included, one on either side of the road. No trench-like segments are included.
- Situation (3): Two LHNS are included, positioned on either side of the road. In addition to this, trench-like segment are added in front of each roadside LHNS.

Case 2 is simply illustrated in Figure 4.2 where the geometry consisted of multiple different segments, each explained from Table 4.2.

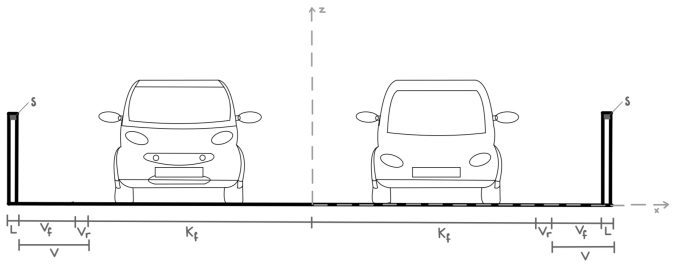

Figure 4.2: Sketch of Case 2 geometry: two-lane road, 40 km/h speed limit.

Table 4.2: Road segments Case 2.

		Width (m)			Height (m)		
		Situation					
Road segment	**Label**	**1**	**2**	**3**	**1**	**2**	**3**
LHNS	L	0.3	0.3	0.3	0	1.1	1.1
Soft top	S	0.3	0.3	0.3	0.05	0.05	0.05
Side shoulder	v_f	0.25	0.25	0.5	0	0	0.05
Side hard shoulder	v_r	0.25	0.25	0.25	0	0	0
Lane	k_f	3.25	3.25	3.25	0	0	0

Case 3: Multiple-lane road with noise barriers separating traffic directions and along the sides.
The third case was based on a multiple-lane road with two lanes in each directions. This case was based on larger roads that go through bigger cities or in the outskirts of urban areas where the vehicle speed is 80 km/h.

- Situation (1): Reference situation. No LHNS or trench-like segments are included.
- Situation (2): Three LHNS are included, two placed on either side of the road and one in the central area between the opposing driving lanes. No trench-like segments are included.
- Situation (3): Three LHNS are included, two placed on either side of the road and one in the central area between the opposing driving lanes. In this situation trench-like segment are added in front of each roadside LHNS as well as on both sides of the LHNS positioned between the opposing driving lanes.

Case 3 is simply illustrated in Figure 4.3 where the geometry consists of multiple different segments, each explained from Table 4.3. As in Case 1, the geometry was simplified in BEM. The simplified geometrical configuration consisted of two vehicles and their adjacent LHNS.

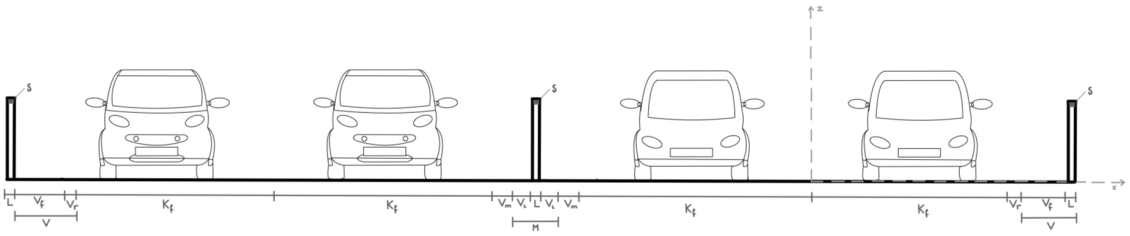

Figure 4.3: Sketch of Case 3 geometry: multiple-lane road, 80 km/h speed limit.

Table 4.3: Road segments Case 3.

		Width (m)			Height (m)		
		Situation					
Road segment	**Label**	**1**	**2**	**3**	**1**	**2**	**3**
LHNS	L	0.3	0.3	0.3	0	1.1	1.1
Soft top	S	0.3	0.3	0.3	0.05	0.05	0.05
Side shoulder	v_f	0.15	0.15	0.5	0	0	0.2–0.5
Side hard shoulder	v_r	0.35	0.35	0.35	0	0	0
Lane	k_f	3.5	3.5	3.5	0	0	0
Central hard shoulder	v_m	0.6	0.6	0.6	0	0	0
Central shoulder	v_l	0	0	0.5	0	0	0.05

4.1 Numerical modelling of BEM compared with analytically calculation

A MATLAB folder including toolboxes, functions and run script will be used for the numerical modelling of BEM. The functions used is created by Jens Forssén and Bart van der Aa, with some modifications made by Patrik Eriksson and Marius Hildén. The run script originally created by Patrik Eriksson and later modified by Marius Hildén [8],[7]. In this thesis, the code will be adapted from train to road traffic applications. This includes changes in setup such as geometry, sound sources and receivers as well as material.

4.1.1 Sound source modelling

Vehicles was modelled as point sources in accordance with the modified Harmonoise source model, with one adjustment. The sources vertical placement (heights) and the vehicles types follow the source model, while a slight modification was made to the horizontal source positions.

Instead of simplifying the model by placing the tyre/road and propulsion sources at a 1 meter distance from the vehicle centre, towards the receiver, this thesis positions two tyre/road sources on either side of the vehicle and the propulsion source in the middle. This adjustment were made due to the implementation of LHNS, when multiple LHNS are applied it might need a more detailed source placement.

Figure 4.4 illustrates a 3D sketch (x-y-z) showing the positions of sources and LHNS for Case 1, 2 and 3. The tyre/road sources (purple) where placed 1.6 meters apart, centred within each driving lane on the x-axes. The propulsion sources (blue) where located midway between the tyre/road sources i.e. 0.8 meters from each on the x-axes. A constant axle width of 1.6 meters is assumed for all vehicle types. The positions of the sources on the z-axes follows the guidelines in Section 2.4.

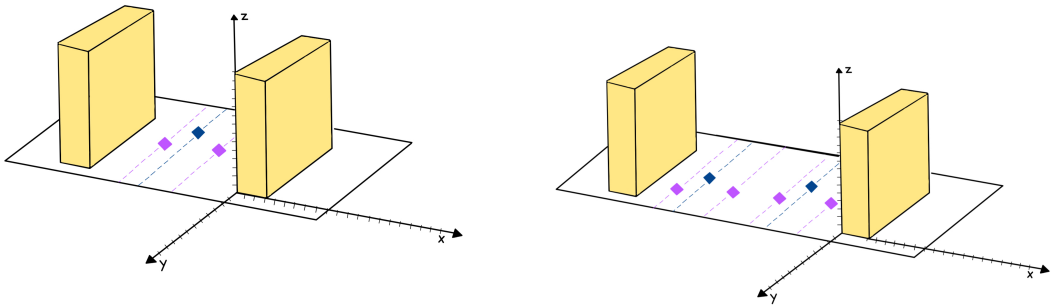

Figure 4.4: 3D sketch of the source placement. The yellow screens represent LHNS, and the blue and purple rhombi represent sound sources. The vehicle are divided into four tyre/road sources (purple) and two propulsion sources (blue). The dashed lines represent the continuation of sound sources along the y-axis, to simulating a moving vehicle. Case 1 is shown on the left, while Cases 2 and 3 are on the right.

Figure 4.5 shows the horizontal plane (x-y) positions of the sources. Each source was aligned along the y-axis and placed at an angular interval of 2 degrees ($\alpha = 2$ %) as seen from the receiver positions covering a range from y = 0 meters to y = 100 meters. By mirroring the setup along the x-axis, an incoherent line sources of 200 meters in the y-axis is formed.

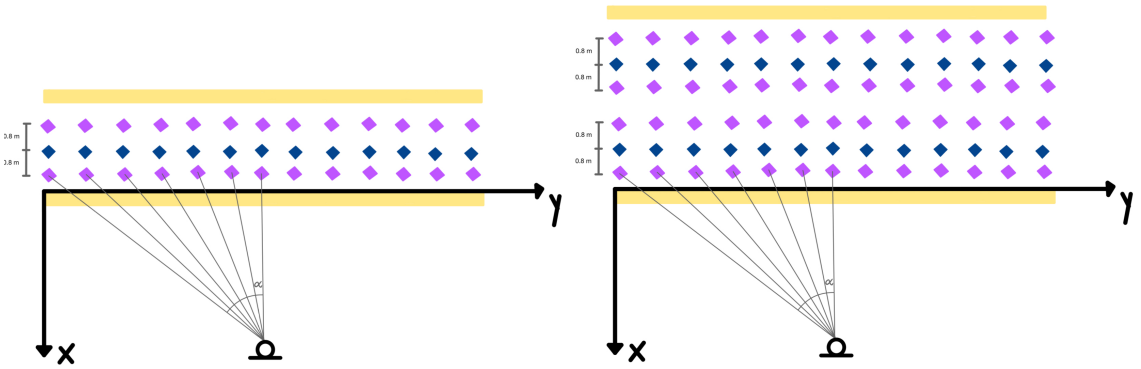

Figure 4.5: View from the top showing source positions (rhombi) in the x–y plane. Tyre/road sources are shown as purple rhombi, and propulsion sources as blue rhombi. Yellow areas indicate the position of the LHNS. The distance between sources are displayed by the gray lines, distance being a 2 % angle, α. Case 1 is shown on the left, while Cases 2 and 3 are on the right.

As stated in Section 2.1, the noise from the tyre/road interaction is directional with a higher sound radiation in the forward direction. This was not accounted for in the application of BEM. All point sources where assumed to be omnidirectional due to the complexity that directivity would introduce in the application of BEM.

4.1.2 Receivers modelling

In order to estimate the sound pressure level in a free field, multiple receiver locations and heights where used. When measuring outdoor sound pressure levels it is recommended to measure at a height of 1.5 meters above the ground [34]. This height

was also applied for the calculations in BEM, along with an additional height of 4 meters to simulate an extra floor. To make the model more robust against interference peaks and dips occurring at specific calculation points, multiple receiver points around 1.5 meters and 4 meters was calculated and then averaged. The clusters of receivers at 1.5 meters and 4 meters where positioned at different distances relative to the sound sources. To evaluate the effects of the LHNS and trench-like segments the receiver was positioned at a distance of 7.5 meters, 15 meters and 30 meters. These distances where chosen to evaluate the effects on both shorter and longer distances where buildings, parks etc could be placed.

4.1.3 Implementation of geometry

The three cases described in Section 4 was implemented in BEM. As mention earlier, each case was evaluated in three situations: (1) without LHNS or trench-like segments, (2) with multiple LHNS but no trench-like segments and (3) with both LHNS and trench-like segments. Situation (1) is handled separately in the post process and not calculated through BEM, see Section 4.1.5.

Case 1: Urban two-lane road with noise barriers separating traffic directions and along the sides.
The first case includes two vehicles and three LHNS. When implementing this geometry in BEM, it was simplified to include only one single vehicle and its adjacent LHNS to reduce computational time. The geometry created and used in BEM are showed in Figure 4.6. The left illustrates situation (2), which includes two LHNS but no trench-like segments. In contrast, the picture on the right displays situation (3), featuring two LHNS along with added trench-like segments.

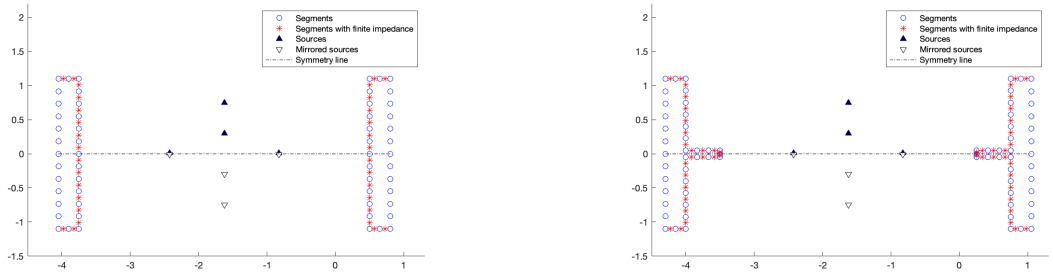

Figure 4.6: Overview of the segmentation and spatial arrangement of sound sources for Case 1. Situation (2) is shown on the left, while situation (3) are on the right.

Case 2: Urban two-lane road with side noise barriers.
The geometry implemented in BEM was identical to the initial sketch and includes two vehicles and two LHNS, see Figure 4.7. The left illustrates situation (2), which includes two LHNS but no trench-like segments while the right figure displays situation (3) which includes trench-like segments as well.

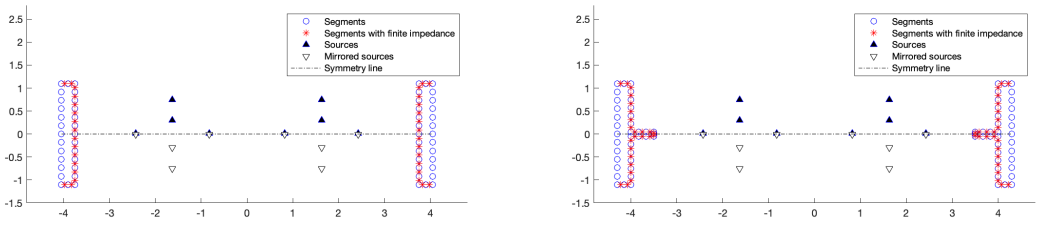

Figure 4.7: Overview of the segmentation and spatial arrangement of sound sources for Case 2. Situation (2) is shown on the left, while situation (3) are on the right.

Case 3: Multiple-lane road with noise barriers separating traffic directions and along the sides.
As in Case 1, the geometry was simplified for the implementation in BEM. The simplified geometrical configuration consisted of two vehicles and their adjacent LHNS, similarly as in Case 2. The geometry created and used in BEM are showed in Figure 4.8. To the left situation (2) is displayed with two LHNS and no trench-like segments, while situation (3) includes trench-like segments.

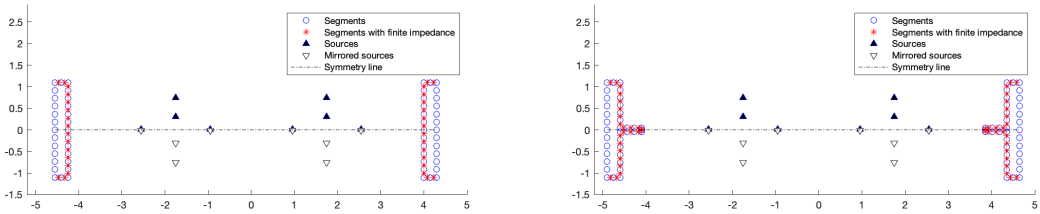

Figure 4.8: Overview of the segmentation and spatial arrangement of sound sources for Case 3. Situation (2) is shown on the left, while situation (3) are on the right.

4.1.4 Materials

Multiple materials for the LHNS and trench-like segments were selected and tested for all three geometry cases described in Section 4. Different impedance models were applied depending on the material and segment. The segments were modelled with finite impedance. Four materials were placed on a hard backing and investigated for the screen: mineral wool in two different thicknesses, Vitrumit and wood wool cement board (**WWCB**). Mineral wool was modelled using the Miki model and the parameters are based on data from the licentiate thesis *Acoustic effect of sound*

absorbing materials and surfaces in road infrastructure by Monica Waaranperä [35]. A mineral wool with a lower flow resistivity was additionally tested. Vitrumit, a material made of glass and flint, was modelled using the Zwikker and Kosten phenomenological model with parameters based on data from the report *Time-domain simulations of low-height porous noise barriers with periodically spaced scattering inclusions* by Bart van der Aa and Jens Forssén [23]. The final material tested for the LHNS was WWCB which was modelled using the Miki model with parameters based on data from the master thesis *WWCB characterizing, modelling and optimizing the sound absorption of wood wool cement boards* by Bram Botterman [36]. The corresponding impedance model parameters are presented in Table 4.4.

Table 4.4: Impedance model parameters used for the LHNS segments.

Material	Impedance model	d (m)	σ (kNs/m^4)	ϕ (-)	k_s (-)
Mineral wool type A	Miki	0.15	22.5	-	-
Mineral wool type A	Miki	0.3	22.5	-	-
Mineral wool type B	Miki	0.15	10	-	-
Mineral wool type B	Miki	0.3	10	-	-
Vitrumit	Zwikker and Kosten	0.1	29.6	0.45	2.84
WWCB	Miki	0.15	5	-	-

A type of lawn and porous asphalt were tested for the trench-like segments. Both materials use the slit-pore model with parameters based on data from the scientific article *Outdoor ground impedance models* by Keith Attenborough, Imran Bashir and Shahram Taherzadeh [20]. The impedance model parameters for the materials are presented in Table 4.5.

Table 4.5: Impedance model parameters used for the trench-like segments.

Material	Impedance model	d (m)	σ (kNs/m^4)	ϕ (-)
Lawn	Slit-pore	0.05	200	0.5
Porous asphalt	Slit-pore	0.05	8	0.2

As a final measure, sedum was implemented on top of the LHNS segments to try to reduce the noise further. Sedum was modelled using the Miki model and the parameters are based on data from the scientific article *Characterisation of the acoustic impedance of vegetated roofs with a multiple-geometry approach* by Chang Liu, Fotis Georgiou and Maarten Hornikx [37]. The impedance model parameters for the materials are presented in Table 4.6.

Table 4.6: Impedance model parameters used for top of the LHNS segments.

Material	Impedance model	d (m)	σ (kNs/m^4)	ϕ (-)
Sedum	Miki	0.05	1.1	-

4.1.5 Processing in BEM

Once the BEM setup was defined, the boundaries of the geometry segments where discretised and the sources was calculated for a defined frequency range of 25 Hz to 5 kHz at the centre frequencies of the third-octave bands. Third-octave bands where used to analyse a more detailed frequency spectrum and to better understand which specific frequencies of the sound are absorbed. This was essential when evaluating the screen's absorption capacity. It is also important for future noise scenarios to know which frequencies are absorbed by the chosen screen material.

In Case 1, where the geometry only include one vehicle between the LHNS, see Section 4, there where four sources that needed to be calculated separately; two tyre/road sources (left and right tyre) and two propulsion sources (light and medium/heavy). For Case 2 and Case 3, where the geometry include two vehicles, see Section 4, the number of sources are doubled, resulting in a total of eight sources being calculated.

After the source calculations, the files where post processed. During the post processing of the BEM modelling, angular translation distances between the source and receiver are introduced, see Figure 4.5. This is necessary because the sources, i.e. the vehicles, are moving objects. If the sound propagation were only analysed at one receiver angle, e.g. directly in front of the vehicle at 0 °, it would not capture the full sound propagation of the sound. By introducing multiple receiver angles, the calculation take into consideration how the sound propagates when a vehicle drives past a receiver.

The final data structure from the BEM calculations include the total sound pressure level $L_{p,tot}$ and direct sound pressure level $L_{p,d}$ for three receiver positions 7.5, 15 and 30 meters, each with two heights, 1.5 and 4 meters. For each receiver-height combination, values are computed and stored for every angle and frequency.

4.1.6 Analytical calculation

To be able to calculate the insertion loss, with the results from BEM, a reference situation without screens or trench-like segments is calculated. This is done with an analytical calculation using a script adapted by Jens Forssén and Bart van der Aa, and later modified by Jens Forssén. The code was then adapted to fit the cases described in this thesis.

Without screen

The sources, receivers and frequency range have the same setup as in BEM. The vehicle distribution was determined based on the type of road being studied. For Case 1 and 2, an urban two lane road with vehicle speed of 40 km/h, were assigned 5 % medium heavy vehicles and 3 % heavy vehicles. Case 3, multiple-lane road with a vehicle speed of 80 km/h, was assigned 1 % medium heavy vehicles and 7 % heavy vehicles.

Each source was assigned a sound power level. The sound power level applied to the vehicles where based on Nord2000. Equations from Section 2.4 and sound power coefficients from Appendix A, were used to assign sound power levels to each source. To predict the sound pressure level at receiver, a refined discretisation along

the source lanes is implemented. The source line ($y = 100$ meters) is divided into smaller sections Δy. Each section Δy acts as a sound source. From traffic flow parameter $\mathrm{N_{perhour}}$, vehicle type distribution $\mathrm{p_i}$, speed limit v and number of source lanes $\mathrm{N_{sourcelanes}}$, a sound power level per meter and per source lane for each vehicle type was calculated, see Equation 4.1. In the equations below, i represents type of vehicle (light, medium or heavy).

$$\Delta L_{\mathrm{W,i}} = 10 \log_{10} \left(\frac{N_{\text{per hour}} \cdot p_{\mathrm{i}}}{1000 \cdot v \cdot N_{\text{source lanes}}} \right) \tag{4.1}$$

The total sound power level for each source type and vehicle type was then calculated, see Equation 4.2. The $L_{\mathrm{W,i,j,single}}$ in the equation is the single vehicle power levels based on the sound power coefficients. These are weighted with a proportional distribution of 80/20 ratio. When calculating for the tyre/road noise, 80 % comes from the tyre/road noise and 20 % from propulsion noise, and vice versa when calculating for the propulsion noise. In the equations below, j represents source type (propulsion or tyre/road).

$$L_{\mathrm{W,i,j}} = 10 \log_{10} \left(0.8 \cdot 10^{L_{\mathrm{W,i,j,single}}/10} + 0.2 \cdot 10^{L_{\mathrm{W,i,j,single}}/10} \right) + \Delta L_{\mathrm{W,i}} \tag{4.2}$$

To account for the amplification of sound reflections of hard ground, a correction is introduced, see Equation 4.3. The reflection coefficient Q assumed to be 1 for hard ground with perfect reflection. The equation also take into account the direct distance $\mathrm{r_{direct,j}}$ and the distance to the receiver from the image source $\mathrm{r_{image,j}}$, see Equation 4.4 and 4.5. These consider the differences in horizontal position (x). lateral distance along the road (y) and height (z).

$$\Delta L_{\mathrm{p,j,hard\ ground}} = 20 \log_{10} \left(\left| 1 + Q \cdot \frac{r_{\mathrm{direct,j}}}{r_{\mathrm{image,j}}} \cdot e^{-jk} \cdot (r_{\mathrm{image,j}} - r_{\mathrm{direct,j}}) \right| \right) \tag{4.3}$$

$$r_{\mathrm{direct,j}} = \sqrt{(x_{\mathrm{source,j}} - x_{\mathrm{receiver,j}})^2 + y^2 + (z_{\mathrm{source}} - z_{\mathrm{receiver}})^2} \tag{4.4}$$

$$r_{\mathrm{image,j}} = \sqrt{(x_{\mathrm{source,j}} - x_{\mathrm{receiver,j}})^2 + y^2 + (z_{\mathrm{source}} + z_{\mathrm{receiver}})^2} \tag{4.5}$$

This correction was considered when calculating the contribution of a single source line for reference condition. The contribution of a single source line, e.g. propulsion noise from heavy vehicles along the whole road, was then calculated for each vehicle type and noise source with Equation 4.6 and 4.7 for reference and free field conditions. An air attenuation factor, $\mathrm{\Delta L_{p,airattenuation}}$ was defined and subtracted from the transfer single source to account for the distance dependent reduction in sound level. The variables $10 \log_{10}(\Delta y)$ is due to discretisation and $10 \log_{10}(2)$ is due to symmetry that only y>0 is the basis.

$$\begin{aligned} \Delta L_{\mathrm{p,transfer,j,REF}} = & -10 \log_{10}(4\pi r^2_{\mathrm{direct,j}}) - \Delta L_{\text{p, air attenuation}} \cdot r_{\mathrm{direct,j}} \\ & + \Delta L_{\mathrm{p,j,hard\ ground}} + 10 \log_{10}(\Delta y) + 10 \log_{10}(2) \end{aligned} \tag{4.6}$$

$$\begin{aligned}\Delta L_{\mathrm{p,transfer,j,FREE}} = & -10 - \Delta L_{\mathrm{p,\ air\ attenuation}} \cdot r_{\mathrm{direct,j}} \\ & + 10\log_{10}(\Delta y) + 10\log_{10}(2)\end{aligned} \tag{4.7}$$

After calculating transfer single source, the equivalent sound energy contribution $\mathrm{w_{eq}}$ from the noise sources where calculated for each vehicle type for reference and free field, see Equation 4.8. This was needed to calculate the equivalent sound pressure level in Equation 4.9 for reference and free field. When summing tyre/road noise for one vehicle, it is represented by two separate positions (i.e. left and right tyre), so the total sound energy from the tyre/road noise sources are assumed to be equally divided between these sources. This means that each tyre/road source was scaled by a factor of 0.5 (i.e. $\beta = 0.5$). The equivalent sound pressure level for propulsion was calculated with the same equations but does not require to be scaled with a 0.5 factor (i.e. $\beta = 1$).

$$w_{\mathrm{eq,i,j}} = 10^{\Delta L_{\mathrm{p,transfer,j}}/10} \tag{4.8}$$

$$\mathrm{L_{eq,i,j}} = 10\log_{10}\left(w_{\mathrm{eq,i,j}} \cdot \beta\right) + L_{W,i,j} \tag{4.9}$$

The final steps before obtaining the equivalent sound pressure levels for reference and free field, for the reference situation without screens or trench, was to sum over multiple variables. First, a summation was done over the road length to account for the sound contributions from all sections of the road, see Equation 4.10.

$$\mathrm{L_{eq,i,j,sum}} = 10\log_{10}\left(\sum 10^{\mathrm{L_{eq,i,j}}/10}\right) \tag{4.10}$$

Next, a summation over source types was performed to obtain the equivalent sound pressure level for each vehicle type and the corresponding number of vehicles, see Equation 4.11.

$$\mathrm{L_{eq,i,sum,1}} = 10\log_{10}\left(\sum 10^{\mathrm{L_{eq,i,j,sum}}/10}\right) \tag{4.11}$$

Then, a summation over vehicle lanes was done, see Equation 4.12. For Case 1, there is only one vehicle while for Case 2 and 3, there is two vehicles that need to be summed together.

$$\mathrm{L_{eq,i,sum,2}} = 10\log_{10}\left(10^{\mathrm{L_{eq,i,sum,1}}/10}\right) \tag{4.12}$$

Finally, summing over the three vehicle types for reference and free field yields the equivalent sound pressure levels $\mathrm{L_{eq}}$ for the reference situation without screens or trench using Equation 4.13.

$$\mathrm{L_{eq,without\ screen}} = 10\log_{10}\left(10^{\mathrm{L_{eq,i,sum,2}}/10}\right) \tag{4.13}$$

With screen, from BEM

Once the reference situation was calculated, the data from BEM is loaded into the script to sum the result over the angles and cluster of receivers for the distances, heights and frequencies. This yields a total sound pressure level $\mathrm{L_{p,tot}}$ and a direct

sound pressure level $L_{p,d}$, each containing one value for each distance and height combination for the frequency range. A correction term $\Delta L_{p,i}$ is then calculated for each source type as the difference between $L_{p,tot}$ and $L_{p,d}$.

For the situation with screen, the calculation follows the same steps as described above. However, the hard ground amplification term $\Delta L_{p,j,hardground}$ is set to zero as it is already accounted for in the calculated correction term from BEM. Including it again would lead to double counting. The correction term $\Delta L_{p,i}$ is then added when calculating the equivalent sound pressure level for reference and free field, see Equation 4.14.

$$L_{eq,i,j} = 10 \log_{10} (w_{eq,i,j} \cdot \beta) + L_{W,i,j} + \Delta L_{p,i} \tag{4.14}$$

The steps after this equation are the same as described above. In the final step the equivalent sound pressure levels L_{eq} for reference and free field with screen are achieved, see Equation 4.15.

$$L_{eq,\text{with screen}} = 10 \log_{10} \left(10^{L_{eq,i,sum}/10}\right) \tag{4.15}$$

4.1.7 Calculation of insertion loss

After the analytical calculations for both the reference situation and the case with screen, the equivalent sound pressure levels L_{eq} for reference and free field where obtained for each scenario. These levels was then A-weighted using standard A-weighting coefficients, see Appendix B. This weighting adjusts the sound levels to better reflect how the human ear perceives the sound. This is relevant because the aim is to reduce the noise levels from the human perspective, thereby contributing to a more sustainable environment. The A-weighted values was then summed across all frequencies, resulting in a single value for each height and distance combination (a total of 6 values). The insertion loss (**IL**) was then calculated as the difference between the A-weighted equivalent without screen $L_{Aeq,withoutscreen}$ and the A-weighted equivalent level with screen $L_{Aeq,withscreen}$ for reference, see Equation 4.16.

$$IL = L_{Aeq,\text{ without screen}} - L_{Aeq,\text{ with screen}} \tag{4.16}$$

4.2 Implementation of noise mapping software

4.2.1 Implementation of geometry

The three cases described in Section 4 was further implemented in a noise mapping software to analyse the effect of LHNS and trench-like segments. The same three situations, as in BEM, were evaluated: (1) without LHNS or trench-like segments. (2) with only LHNS, and (3) with both LHNS and trench-like segments. The same cases were used to facilitate a consistent comparison and evaluation of the result against BEM.

Case 1: Urban two-lane road with noise barriers separating traffic directions and along the sides.
In the noise mapping software, the full geometry was used without any simplification. For Case 1 all vehicles, LHNS and trench-like segments initially defined were modelled, in contrast to BEM where the geometry was simplified to include one vehicle instead of two, and two LHNS instead of three. In addition all three situations were modelled in the noise mapping software, compared to BEM where situation (1) where handled analytically. The geometries for Case 1 are shown in Figure 4.9. For situation (1), the LHNS (shown in blue) are absent, while they are present in situation (2) and (3). In situation (3), there are additional trench-like segments between the roads and LHNS, although these are not displayed in the figure.

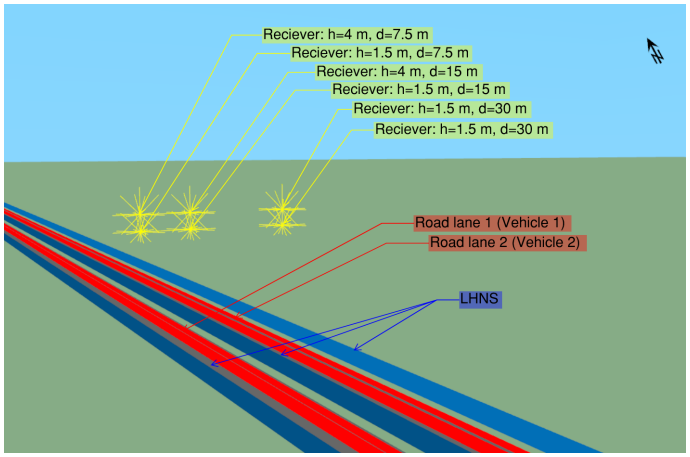

Figure 4.9: 3D model of Case 1 geometry in SoundPLAN. The blue barriers represents LHNS, red lines are roads (sound sources) and the yellow clusters are receivers at 2 different heights and three different distances.

Case 2: Urban two-lane road with side noise barriers.
For Case 2, the full geometry was used in the noise mapping software identical to the implementation in BEM. It contains two LHNS and two vehicles. All situations were handled in the noise mapping software as Case 1. The geometries for Case 1 are shown in Figure 4.10. For situation (1), the LHNS (shown in blue) are absent, while they are present in situation (2) and (3). In situation (3), there are additional trench-like segments between the road and LHNS, although these are not displayed in the figure.

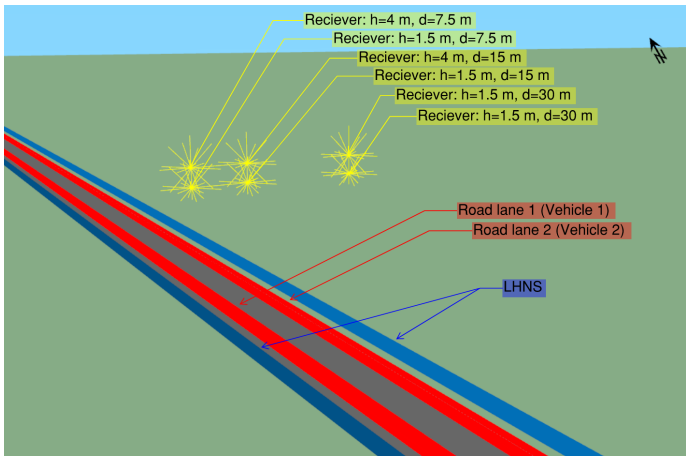

Figure 4.10: 3D model of Case 2 geometry in SounsPLAN. The blue barriers represents LHNS, red lines are roads (sound sources) and the yellow clusters are receivers at 2 different heights and three different distances.

Case 3: Multiple-lane road with noise barriers separating traffic directions and along the sides.
For Case 3, the complete geometry with four vehicles, three LHNS and trench-like segments was used without simplification in the noise mapping software. This implementation is different from BEM, where the geometry where reduced to two vehicles and two LHNS. As with the other cases, all three situations were modelled in the noise mapping software. The geometries for Case 1 are shown in Figure 4.11. For situation (1), the LHNS (shown in blue) are absent, while they are present in situation (2) and (3). In situation (3), there are additional trench-like segments between the roads and LHNS, although these are not displayed in the figure.

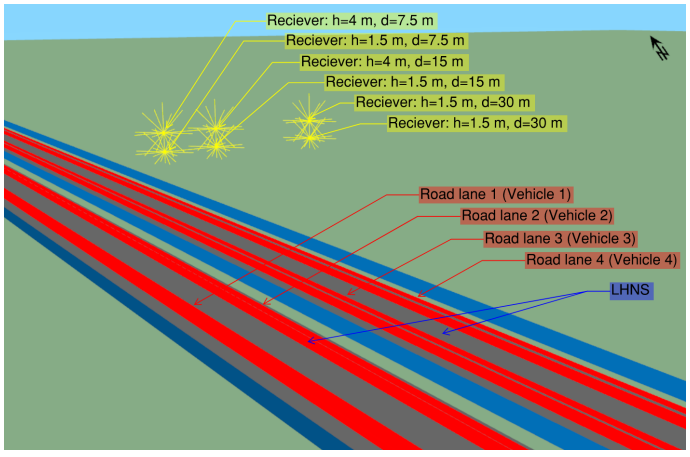

Figure 4.11: 3D model of Case 3 geometry in SoundPLAN. The blue barriers represents LHNS, red lines are roads (sound sources) and the yellow clusters are receivers at 2 different heights and three different distances.

Gibraltarvallen

In the final step of the evaluation, one selected LHNS and trench geometry where applied to a realistic urban scenario. The chosen location, Gibraltarvallen, is situated in central Gothenburg where new residential and commercial building are planned. A two-lane road called Gibraltargatan, with a speed limit of 50 km/h, runs through this area. This road was a good candidate to implement one of the studied geometries, especially Case 2. There are space on both sides of Gibraltargatan to introduce absorptive LHNS without having to change the road itself. The road also has two lanes with a lane width of approximately 3.25 m, the same lane width defined for Case 2. An overview of the area and the test road are displayed in Figure 4.12.

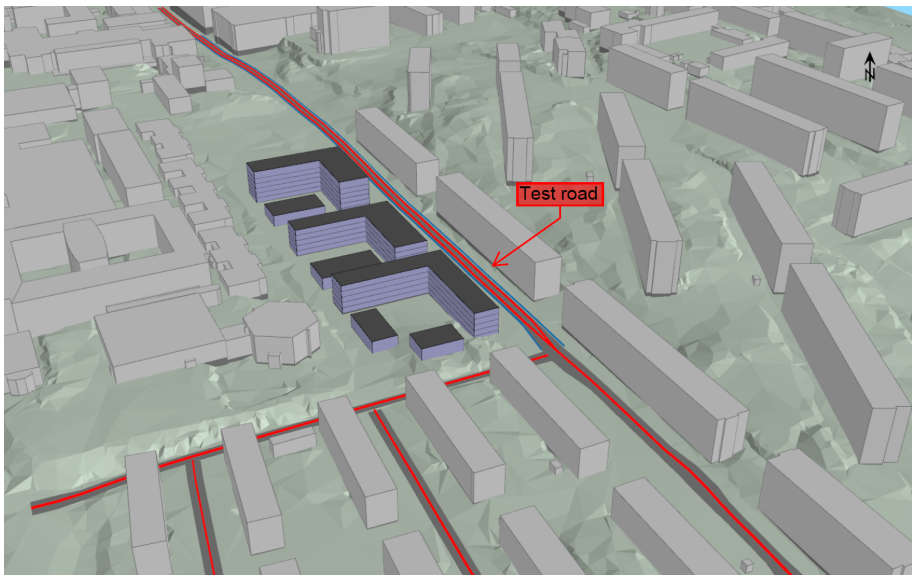

Figure 4.12: Overview of Gibraltarvallen, test road for multiple absorptive LHNS marked with red label.

Due to the characteristics of Gibraltargatan, the geometry for Case 2 defined in Section 4 was be used without adaptations. Based on insights gain from modelling the three cases described above, only two of the situations described in Chapter 4 were implemented in the real case application: (1) a reference case without LHNS or trench-like segments and (2) a setup with two LHNS placed on either side of the road with no trench-like segments included. For the implementation of the reference situation (1), no changes of the built geometry in SoundPLAN where changed. When implementing the absorptive LHNS, barriers where simply added to both sides of the road. To evaluate the effects of the LHNS, a residential building, 7 floors, located 12.5 meters from the road was studied. The geometry of both situations, with and without LHNS is displayed in Figure 4.13. Additionally, a situation with one LHNS closest to the studied building was implemented.

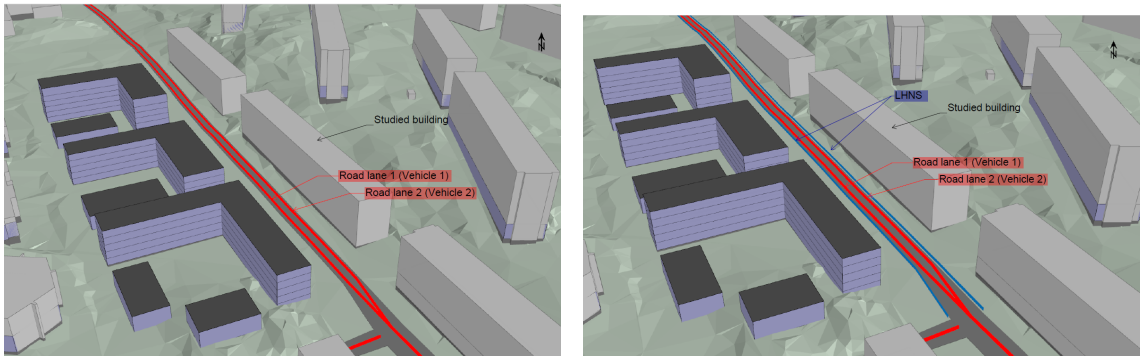

Figure 4.13: 3D model of Gibraltarvallen with a zoomed view of the studied building. The blue barriers represents LHNS and the red lines are the road (sound sources). Situation (1), reference, is shown of the left, while situation (2) are displayed on the right.

4.2.2 Materials

The same materials were implemented for BEM and in the noise mapping software SoundPLAN. In SoundPLAN however, impedance models was not used in the same way as in BEM. Instead, when LHNS and trench-like segments where defined in the software, they needed an sound absorption coefficient for the assumed material. Plane wave reflection at a boundary with normal incidence was assumed and the absorption coefficient was calculated from the pressure reflection coefficient using the equations described in Section 2.2. The software cannot create barriers where the top of the screen is defined as a different material, which means that sedum was not included in the calculations in SoundPLAN. In addition to the defined material absorption coefficient for the absorption segments, the surfaces of the remaining area was assumed to be hard ($\underline{r} = -1$). The calculated pressure reflection coefficients $\underline{r}$ and sound absorption coefficients α are presented in Table 4.7. The absorption coefficients for mineral wool and WWCB was automatically rounded off to 1 in the software. They where therefore implemented as one and the same material, decreasing number of screen materials tested to two (Vitrumit and mineral wool/WWCB). All material combinations were tested in each of the three road cases. In the real case scenario implemented at Gibraltarvallen, only the mineral wool/WWCB screen material with no trench-like segments where implemented.

Table 4.7: Pressure reflection coefficients and sound absorption coefficients for the materials

Material	$\underline{r}$ (-)	α (-)
Mineral wool type A (0.15m)	0.0927+0.1103i	0.9793
Mineral wool type A (0.30m)	0.0927+0.1103i	0.9793
Mineral wool type B (0.15m)	0.0535+0.0709i	0.9921
Mineral wool type B (0.30m)	0.0544+0.0711i	0.9920
Vitrumit	0.5185+0.1008i	0.7209
WWCB	0.0338+0.0581i	0.9955
Porous asphalt	0.4271+0.1205i	0.8030
Lawn	0.5161+0.163i	0.7070

When defining ground absorption, it was also necessary to specify the effective flow resistivity. SoundPLAN includes a predefined set of ground categories, each with a specific flow resistivity. Based on the values used in BEM, and of the calculation of sound absorption coefficients, the most similar category were used. The used flow resistivity values are presented in Table 4.8.

Table 4.8: Impedance model parameters used for the trench-like segments

	Flow resistivity, (kNs/m^4)	
Material	BEM	SoundPLAN
Lawn	200	200 (N2K:D:normal uncompacted ground)
Porous asphalt	8	10 (TNM: Powder snow)

4.2.3 Simulations and data analysis

In order to process the geometry in SoundPLAN a few parameters had to be set. In SoundPLAN it was possible to map sound with many different standards. In this thesis, the standard used was Nord2000, which uses a frequency range of 25 Hz to 10 kHz at the centre frequencies of the third-octave bands. The sound sources (roads) were assigned traffic data based on the road type. The vehicle distribution was set to the same values as in BEM, the roads were also assigned an annual average daily traffic (AADT) value, see Table 4.9. The traffic distribution was based on road type, each presented in Table 4.9. The road surface was set to SMA 11 and $L_{\mathrm{AFmax,n}}$ was evaluated for n=6 for all cases.

Table 4.9

Case	Road type	AADT	% medium heavy vehicles	% heavy vehicles
1	SE type D	5600	5	3
2	SE type D	5600	5	3
3	SE type B	36789	1	7
Real case	SE type D	5600	5	3

The receivers for Case 1, 2 and 3 were set to single point receivers at a height of 1.5 meters and 4 meters for all three distances, 7.5 meters, 15 meters and 30 meters. For the implementation of a real case, a buildings facade was used as the receiver to better simulate the impact of absorptive LHNS in a real urban setting. The building was set to 19.6 meters, divided into 7 floors. The receivers height on the buildings facade was set to 1.5 meters to better compare with the results from BEM. The reflection loss, for the facade, was set to 1 dB.

For SoundPLAN to run the simulations, additional settings was specified. The reflection order was set to 3 when evaluating single point sound (for Case 1, 2 and 3) as well as for the evaluations of the facade noise map in the implementation of the real case scenario. When evaluating the real case scenario with a grid map, the reflection order was set to 2. The grid map resolution was set to 5 and the receivers heights was set to 2 meter above ground.

From the simulations the assessments chosen to evaluate was $L_{\mathrm{Aeq,24h}}$ and $L_{\mathrm{Amax,road}}$. From these assessments one can determine the impact of the absorptive LHNS and trench-like segments for each geometry. To evaluate the influence more easily, the insertion loss was determined. The insertion loss for both the A-weighted equivalent sound level over 24 hours and the the maximum sound pressure level from road traffic was calculated with equation 4.17 and 4.18. In the real case scenario, facade noise maps and grid maps were produced rather.

$$\mathrm{IL} = L_{\mathrm{Aeq,\,24h,\,without\,screen}} - L_{\mathrm{Aeq,\,24h,\,with\,screen}} \tag{4.17}$$

$$\mathrm{IL_{Amax}} = L_{\mathrm{Amax,\,road,\,without\,screen}} - L_{\mathrm{Amax,\,road,\,with\,screen}} \tag{4.18}$$

5
Results

5.1 Insertion loss and SPL obtained from BEM

The IL from BEM calculations, for all three cases, are presented below and can be observed in Table 5.1, 5.2 and 5.3. When comparing the three cases, a general increase in IL can be observed at the lower receiver position 1.5 meters between distances 7.5 and 15 meters, followed by a decrease at 30 meters. For Case 1 and Case 2, the IL at 30 meters is the lowest value at the 1.5 meters receiver position. For Case 3, the IL at 30 meters is similar to that at 7.5 meters. For the higher receiver position (4 meters), a general trend of increasing IL with increasing distance is observed for all three cases. This may be due to entering the barrier's shadow zone.

The results for hard screens show a similar trend for both receiver heights. However, at the 1.5 meters receiver position, the IL is approximately half that of the absorptive LHNS, and it is significantly lower also at the 4 meters receiver position. These results suggest that hard screens are significantly less effective than absorptive LHNS. When comparing the same LHNS material with different trench-like segments within each case, they yield almost the exact same insertion loss. This indicates that the choice of material tested of the trench-like segments do not matter. Furthermore, removing the trench-like segments, allowing a narrower placement of the screens, results in an increase of IL for all LHNS material tested. It can also be observed across all cases that mineral wool type A obtain the same results regardless of thickness. In contrast, mineral wool type B, which has a lower flow resistivity, shows some variations with thickness. An IL difference of around 0.1–0.8 dB is noted for mineral wool type B across all three cases, which is not so significant. Mineral wool type B also shows better IL than type A, indicating that the material with lower flow resistivity could be more beneficial to use. The highest IL values for all three cases are obtained with no trench in combination with mineral wool type B or WWCB. These combinations show similar IL with minor deviations at some distances. For all cases, it can be seen that at the lower receiver position (1.5 meters), there is almost no decrease in IL with increasing distance.

Case 1 and 2 handle the same traffic situation, the difference being a third screen implemented between the driving lanes in Case 1. The results show that adding a third LHNS increases the insertion loss by approximately 0.5–3.5 dB, depending on receiver position and situation. Among the three cases, Case 1 shows the highest IL at the 4 meters receiver position. Among the three cases, Case 3 shows the highest IL at the low receiver position. This may partly be explained by the fact that tyre/road noise becomes more dominate when the speed increases.

			IL [dB]		
Trench	**LHNS**	**Height**	**Distance 7.5 m**	**Distance 15 m**	**Distance 30 m**
Porous asphalt	Vitrumit	1.5 m	9.9	10.3	8.2
		4 m	4.3	7.1	8.9
Porous asphalt	Mineral wool type A (0.15 m)	1.5 m	11.3	12.0	9.9
		4 m	6.0	8.9	11.2
Porous asphalt	Mineral wool type A (0.3 m)	1.5 m	11.3	12.0	9.9
		4 m	6.0	8.9	11.2
Porous asphalt	Mineral wool type B (0.15 m)	1.5 m	11.3	12.1	9.9
		4 m	6.0	8.9	11.2
Porous asphalt	Mineral wool type B (0.3 m)	1.5 m	11.8	12.7	10.7
		4 m	6.5	9.5	12.1
Porous asphalt	WWCB	1.5 m	11.6	12.3	10.3
		4 m	6.6	9.5	11.6
Lawn	Vitrumit	1.5 m	10.0	10.4	8.4
		4 m	4.3	7.1	8.9
Lawn	Mineral wool type A (0.15 m)	1.5 m	11.3	12.1	10.0
		4 m	6.0	8.9	11.2
Lawn	Mineral wool type A (0.3 m)	1.5 m	11.3	12.1	10.0
		4 m	6.0	8.9	11.2
Lawn	Mineral wool type B (0.15 m)	1.5 m	11.6	12.4	10.4
		4 m	6.5	9.4	11.7
Lawn	Mineral wool type B (0.3 m)	1.5 m	11.9	12.8	10.7
		4 m	6.5	9.5	12.1
Lawn	WWCB	1.5 m	11.6	12.3	10.4
		4 m	6.6	9.5	11.7
-	Vitrumit	1.5 m	10.3	10.7	8.8
		4 m	4.6	7.4	9.7
-	Mineral wool type A (0.15 m)	1.5 m	11.7	12.3	10.3
		4 m	6.6	9.3	11.7
-	Mineral wool type A (0.3 m)	1.5 m	11.7	12.4	10.3
		4 m	6.6	9.3	11.8
-	Mineral wool type B (0.15 m)	1.5 m	12.1	12.7	10.6
		4 m	7.2	9.8	12.0
-	Mineral wool type B (0.3 m)	1.5 m	12.3	13.0	10.9
		4 m	7.3	10.0	12.5
-	WWCB	1.5 m	12.1	12.5	10.6
		4 m	7.4	10.0	11.9
-	Hard screen	1.5 m	6.54	6.6	5.1
		4 m	0.4	2.2	4.2

Table 5.1: Insertion loss for Case 1.

			IL [dB]		
Trench	**LHNS**	**Height**	**Distance 7.5 m**	**Distance 15 m**	**Distance 30 m**
Porous asphalt	Vitrumit	1.5 m	9.8	10.3	8.6
		4 m	2.6	5.8	8.3
Porous asphalt	Mineral wool type A (0.15 m)	1.5 m	10.6	11.4	9.6
		4 m	3.3	7.2	10.0
Porous asphalt	Mineral wool type A (0.3 m)	1.5 m	10.7	11.5	9.6
		4 m	3.3	7.2	10.0
Porous asphalt	Mineral wool type B (0.15 m)	1.5 m	10.7	11.4	9.6
		4 m	3.3	7.2	10.0
Porous asphalt	Mineral wool type B (0.3 m)	1.5 m	11.2	12.0	10.2
		4 m	3.	7.	10.6
Porous asphalt	WWCB	1.5 m	10.9	11.6	9.9
		4 m	3.5	7.6	10.3
Lawn	Vitrumit	1.5 m	9.9	10.4	8.7
		4 m	2.6	5.9	8.3
Lawn	Mineral wool type A (0.15 m)	1.5 m	10.7	11.5	9.7
		4 m	3.3	7.2	10.0
Lawn	Mineral wool type A (0.3 m)	1.5 m	10.7	11.5	9.7
		4 m	3.3	7.2	10.0
Lawn	Mineral wool type B (0.15 m)	1.5 m	10.9	11.7	10.0
		4 m	3.5	7.5	10.3
Lawn	Mineral wool type B (0.3 m)	1.5 m	11.0	11.9	10.1
		4 m	3.5	7.6	10.5
Lawn	WWCB	1.5 m	10.8	11.5	9.9
		4 m	3.2	7.5	10.3
-	Vitrumit	1.5 m	9.9	10.2	8.6
		4 m	2.5	5.6	8.1
-	Mineral wool type A (0.15 m)	1.5 m	10.9	11.5	9.8
		4 m	3.5	7.4	10.2
-	Mineral wool type A (0.3 m)	1.5 m	10.9	11.5	9.7
		4 m	3.5	7.4	10.2
-	Mineral wool type B (0.15 m)	1.5 m	11.2	11.9	10.2
		4 m	3.8	7.8	10.7
-	Mineral wool type B (0.3 m)	1.5 m	11.3	12.1	10.3
		4 m	3.8	7.9	10.9
-	WWCB	1.5 m	11.2	11.8	10.2
		4 m	3.8	7.9	10.7
-	Hard screen	1.5 m	5.1	5.6	4.3
		4 m	0.1	0.4	1.2

Table 5.2: Insertion loss for Case 2.

			IL [dB]		
Trench	**LHNS**	**Height**	**Distance 7.5 m**	**Distance 15 m**	**Distance 30 m**
Porous asphalt	Vitrumite	1.5 m	11.1	12.7	11.1
		4 m	2.3	5.9	9.2
Porous asphalt	Mineral wool type A (0.15 m)	1.5 m	12.0	13.9	12.1
		4 m	2.8	7.6	11.3
Porous asphalt	Mineral wool type A(0.3 m)	1.5 m	12.0	13.9	12.1
		4 m	2.8	7.6	11.3
Porous asphalt	Mineral wool type B (0.15 m)	1.5 m	12.0	13.9	12.1
		4 m	2.8	7.6	11.3
Porous asphalt	Mineral wool type B (0.3 m)	1.5 m	12.3	14.3	12.5
		4 m	3.0	8.0	11.9
Porous asphalt	WWCB	1.5 m	12.3	14.3	12.6
		4 m	2.9	8.0	11.9
Lawn	Vitrumit	1.5 m	11.2	12.7	11.2
		4 m	2.3	5.9	9.2
Lawn	Mineral wool type A (0.15 m)	1.5 m	12.1	13.9	12.2
		4 m	2.8	7.6	11.3
Lawn	Mineral wool type A (0.3 m)	1.5 m	12.1	13.9	12.2
		4 m	2.8	7.6	11.3
Lawn	Mineral wool type B (0.15 m)	1.5 m	12.3	14.2	12.6
		4 m	2.9	7.9	11.8
Lawn	Mineral wool type B (0.3 m)	1.5 m	12.3	14.3	12.6
		4 m	2.9	8.0	11.8
Lawn	WWCB	1.5 m	12.3	14.2	12.6
		4 m	2.9	8.0	11.9
-	Vitrumit	1.5 m	11.1	12.5	11.0
		4 m	2.3	5.8	8.9
-	Mineral wool type A (0.15 m)	1.5 m	12.3	14.1	12.2
		4 m	3.2	7.9	11.4
-	Mineral wool type A (0.3 m)	1.5 m	12.3	14.1	12.2
		4 m	3.2	7.9	11.4
-	Mineral wool type B (0.15 m)	1.5 m	12.6	14.5	12.7
		4 m	3.4	8.4	12.0
-	Mineral wool type B (0.3 m)	1.5 m	12.7	14.6	12.7
		4 m	3.4	8.4	12.1
-	WWCB	1.5 m	12.7	14.6	12.8
		4 m	3.5	8.5	12.2
-	Hard screen	1.5 m	6.1	7.1	6.2
		4 m	0.0	0.8	2.8

Table 5.3: Insertion loss for Case 3.

The A-weighted SPL in 1/3 octave band, for all three cases, at a distance 15 meters and receiver height 1.5 meters, are presented in 5.1, 5.2 and 5.3. The IL is shown as the gap between the reference curve and the curve of interest. For Case 1, the IL starts around 63 Hz, compared to Cases 2 and 3 which starts closer to 100 Hz. A significant IL of 10 dB occurs for Case 1 and 2 after 315 Hz, in contrast to Case 3 where 10 dB is achieved after 400 Hz.

In Case 1, there is a peak around 80 Hz , especially prominent when trench-like segments are included. This peak is less noticeable in Case 2 but still there, while in Case 3 it does not appear. Instead a different peak, earlier at 50 Hz can be observed instead, mainly visible at a distance of 30 meters and receiver height 1.5 meters (see Figure 5.6). The origin of the 80 Hz peak may be due to propulsion noise, which tends to dominate at that frequency. This peak shows how difficult it is to reduce propulsion noise, especially for case 1 and 2. The origin of the peak at 50 Hz for case 3 is unknown. It's also clear that Vitrumit performs worse than both mineral wool and WWCB across the entire frequency range. However, the difference between

mineral wool and WWCB is small, and their performance is quite similar across all frequencies.

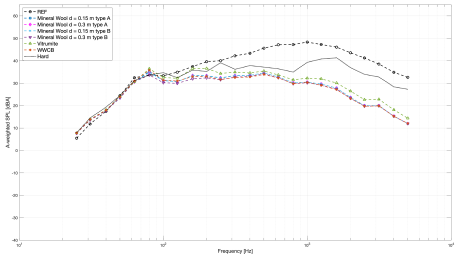

(a) Trench-like segment: Porous asphalt

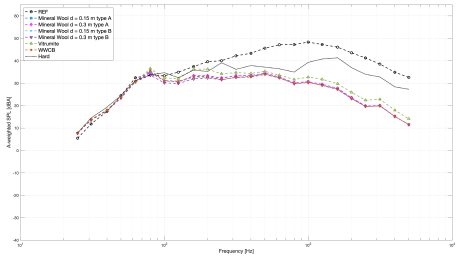

(b) Trench-like segment: Lawn

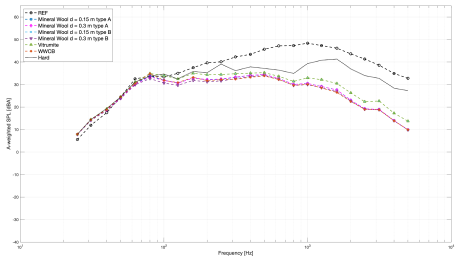

(c) Trench-like segment: None

Figure 5.1: A-weighted SPL for Case 1, showing all different trench and absorptive LHNS configurations. Receiver height: 1.5 meters above ground. Distance: 15 meters from source.

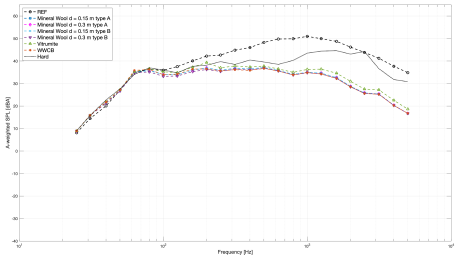

(a) Trench-like segment: Porous asphalt

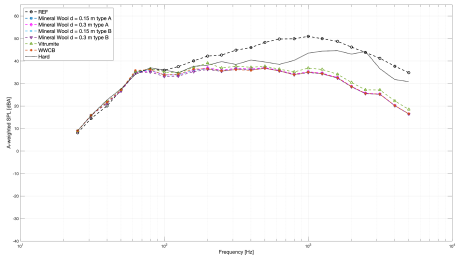

(b)Trench-like segment: Lawn

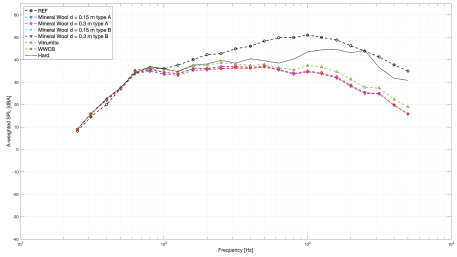

(c) Trench-like segment: None

Figure 5.2: A-weighted SPL for Case 2, showing all different trench and absorptive LHNS configurations. Receiver height: 1.5 meters above ground. Distance: 15 meters from source.

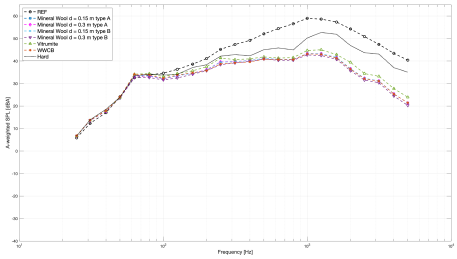

(a) Trench-like segment: Porous asphalt

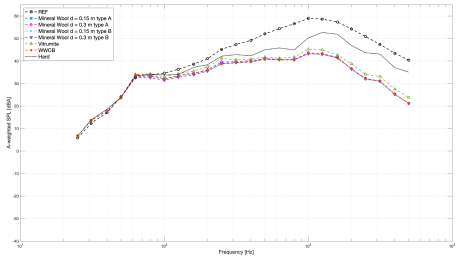

(b) Trench-like segment: Lawn

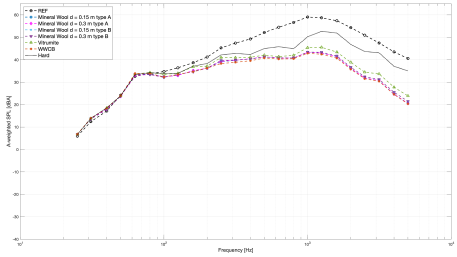

(c) Trench-like segment: None

Figure 5.3: A-weighted SPL for Case 3, showing all different trench and absorptive LHNS configurations. Receiver height: 1.5 meters above ground. Distance: 15 meters from source.

The A-weighted SPL in 1/3 octave band, for Cases 1, 2 and 3, at a receiver height of 1.5 meters and varying distances, is shown to illustrate the varying frequency content, see Figure 5.4, 5.5 and 5.6. For all three cases, it is evident that at shorter distances (7.5 meters), the IL is higher in the lower frequency range (100 Hz to 630 Hz) compared to longer distances (30 meters). However for longer distances, the IL is slightly higher compared to shorter distances.

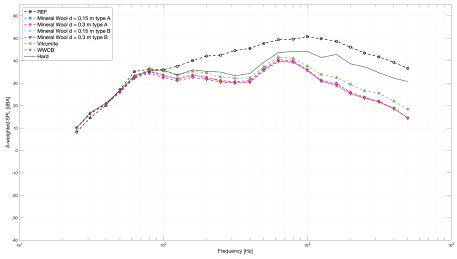

(a) Distance: 7.5 meters

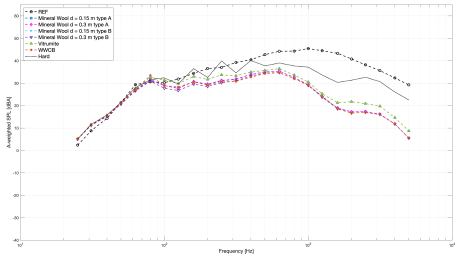

(b) Distance: 30 meters

Figure 5.4: A-weighted SPL for Case 1, without trench-like segments. Receiver height: 1.5 meters above ground.

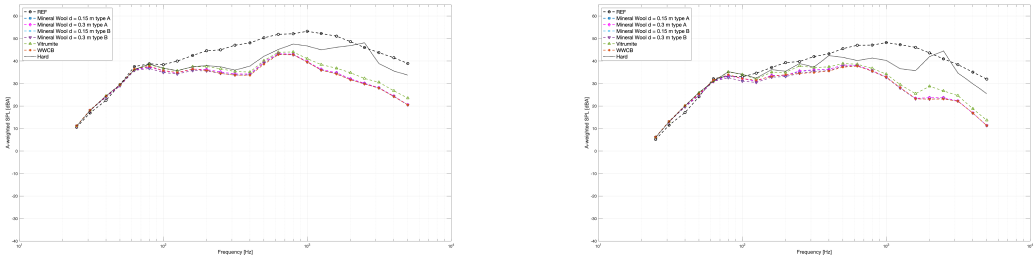

(a) Distance: 7.5 meters (b) Distance: 30 meters

Figure 5.5: A-weighted SPL for Case 2, without trench-like segments. Receiver height: 1.5 meters above ground.

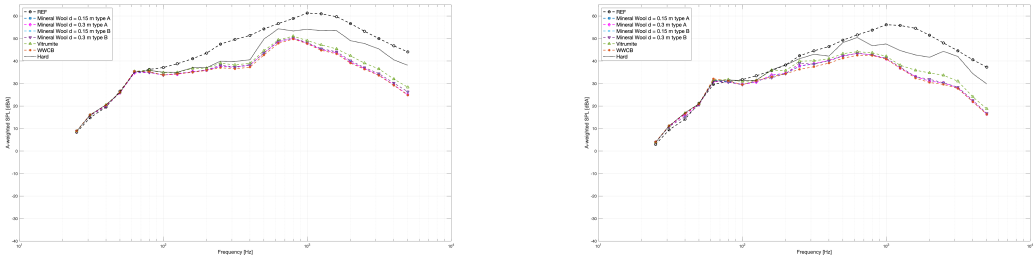

(a) Distance: 7.5 meters (b) Distance: 30 meters

Figure 5.6: A-weighted SPL for Case 3, without trench-like segments. Receiver height: 1.5 meters above ground.

5.2 Noise mapping software

5.2.1 Insertion loss and SPL obtained from Case 1, 2 and 3

The following section presents the IL obtain from simulations in SoundPLAN for all three cases and their various configurations of absorptive LHNS and trench-like segments. The obtained IL from all three cases can be observed in Table 5.4, 5.5 and 5.6.

The initial focus is to observe the similarities of the three cases. A general increase of IL can be observed for multiple absorptive LHNS, such as Vitrumit, mineral wool and WWCB compared to hard reflective screens, see Table 5.4, 5.5 and 5.6. The results show that hard screens provide little to no IL, even suggesting a negative IL at further distances. One possible explanation could be the reflection order. For all cases and materials the reflection order was set to 3. Since a hard barrier reflects more energy than an absorptive one, the reflections might reach the receiver in different paths. The result suggest that hard screens modelled in SoundPLAN are sensitive to the reflection order setting, which may affect the results. It is also evident, that materials such as mineral wool and WWCB performs better that Vitrumit across all height and distances studied. This can be observed, for instance, in the IL for the geometry that exclude trench-like segments. It shows an IL of

7.5 dB for mineral wool/WWCB at a height of 1.5 meters and at a distance of 7.5 meters compared to 4.8 dB for Vitrumit, see Case 2 presented in Table 5.5.

The effects of ground material of trench-like segments on the IL are very limited, if not absent. The difference between IL with trench-like segments made of lawn or porous asphalt are at most 0.1 dB, only occurring when Vitrumit is selected as LHNS, see Table 5.4, 5.5 and 5.6. Due to the small difference of 0.1 dB, the choice of trench material appears to have no significant impact on the IL. The ground materials has little to no effects, while the trench geometry seems to play an more important role. When removing the trench-like segments, enabling a closer placement of the absorptive LHNS to the roads, the IL is increased, see 5.4, 5.5 and 5.6. This can be observed for all cases, most prominent in Case 1 for screen material Mineral wool/WWCB, with an increase of maximum 1.1 dB, see Table 5.4. It is evident that removing the trench-like segment leads to an increase in IL, suggesting that trench-like segments would be ineffective as a NRD. This also suggest that the placement of the LHNS is critical, where placing the LHNS closer to the sound source results in higher IL.

The next focus is to observe the effects of distance and height on the IL. For the lower set receiver, 1.5 meters, it can be observed that IL decreases as the distance becomes larger, see 5.4, 5.5 and 5.6. The decrease over distance is most prominent for screen material Vitrumit. For Case 2, without trench, Vitrumit decreases 2.1 dB at receiver 1.5 meters between 7.5 meters and 30 meters distance, while mineral wool/WWCB only decreases with 1.3 dB at the same distances.

For the higher receiver, 4 meters, the same trend can not be observed. For Case 1, the IL varies, but are always the highest at 7.5 meters distance for screen material Vitrumit. However for Case 2 and 3 the IL, for the higher receiver, behaves differently. The IL for Vitrumit is always the lowest at the shortest distance. A contradiction to Case 1, possibly suggesting uncertainties in the simulation. In Case 1, where multiple LHNS are placed closer together, it is known that SoundPLAN might have difficulties accurately modelling screens, which could indicate simulation errors.

For screen material mineral wool/WWCB it is evident, for Case 1, that the IL is always the lowest at a distance of 7.5 meters and peaks at 15 meters. For Case 2 and 3 the IL is also lowest at 7.5 meters but instead of peaking at 15 meters it gradually increases over distance and peaks at 30 meters. The IL being higher at larger distances could potentially be due to the placement of the receiver. It is located well above the screen height, reducing the LHNS ability to block the direct sound path which could potentially lead to a decrease in IL at shorter distances.

For the receiver position, at height 1.5 meters, IL_{max} decreases with increasing distance from the source. For the higher receiver position, 4 meters, the IL_{max} increases with distance from the source. This could potentially be caused by the receiver being in the acoustic shadow zone. Additionally, IL_{max} varies between being higher and lower than the IL. The cause of this inconsistent behaviour is unknown and was not investigated further.

Case 1 and 2 handle the same traffic situation, the difference being a third screen implemented between the driving lanes in Case 1. The results show that adding a third LHNS increases the insertion loss by approximately 2–6 dB, depending on

receiver position and situation. Case 1 also shows the highest IL for all three cases. The slightly better IL results of Case 3 compared to Case 2 could be due to an increased speed limit in Case 3, which results in more dominant tyre/road noise. However, it's important to note that SoundPLAN might not properly handle more than two screens, which could affect the accuracy of the results obtained.

			IL/IL$_{Amax}$ [dB]		
Trench	**LHNS**	**Height**	**Distance 7.5 m**	**Distance 15 m**	**Distance 30 m**
Porous asphalt	Vitrumit	1.5 m	6.8/8.5	5.8/8	5.2/7
		4 m	5.3/4.9	4.9/6.1	5.1/6.4
Porous asphalt	Mineral wool and WWCB	1.5 m	10.2/10.7	9.6/10.5	9.1/9.8
		4 m	8.4/5.9	10.1/8.9	9.9/9.6
Lawn	Vitrumit	1.5 m	6.8/8.4	5.8/8.0	5.1/6.9
		4 m	5.3/4.8	5.0/6.0	5.0/6.3
Lawn	Mineral wool and WWCB	1.5 m	10.2/10.6	9.6/10.5	9.1/9.8
		4 m	8.4/5.8	10.1/8.9	9.9/9.6
-	Vitrumit	1.5 m	7.2/8.7	6.2/8.2	5.5/7.0
		4 m	5.4/5.7	5.1/6.5	5.4/6.6
-	Mineral wool and WWCB	1.5 m	11.0/11.2	10.3/10.9	9.8/10.1
		4 m	9.5/7.2	11.0/9.8	10.6/10.2
-	Hard screen	1.5 m	1.2/4.8	-0.1/3.7	-1.0/1.8
		4 m	1.1/3.5	-0.7/2.1	-1.2/1.3

Table 5.4: Insertion loss for Case 1.

			IL/IL$_{Amax}$ [dB]		
Trench	**LHNS**	**Height**	**Distance 7.5 m**	**Distance 15 m**	**Distance 30 m**
Porous asphalt	Vitrumit	1.5 m	4.6/8.4	3.4/7.0	2.6/5.3
		4 m	2.0/2.0	3.3/2.9	2.6/3.5
Porous asphalt	Mineral wool and WWCB	1.5 m	7.0/9.7	6.3/8.5	5.9/7.0
		4 m	2.5/2.2	5.0/3.6	6.2/5
Lawn	Vitrumit	1.5 m	4.6/8.3	3.4/6.9	2.5/5.2
		4 m	1.9/1.9	3.3/2.8	2.6/3.4
Lawn	Mineral wool and WWCB	1.5 m	7.0/9.7	6.3/8.5	5.9/7.0
		4 m	2.5/2.2	5.0/3.6	6.2/5
-	Vitrumit	1.5 m	4.8/8.5	3.5/7.0	2.7/5.4
		4 m	2.1/2.0	3.5/2.9	2.6/3.6
-	Mineral wool and WWCB	1.5 m	7.5/9.9	6.7/8.6	6.2/7.2
		4 m	2.7/2.3	5.5/3.9	6.5/5.3
-	Hard screen	1.5 m	-0.1/5.1	-2.1/3.4	-3.1/1.1
		4 m	0.9/1.3	0.4/1.3	-2.3/0.5

Table 5.5: Insertion loss for Case 2.

			IL/IL$_{Amax}$ [dB]		
Trench	**LHNS**	**Height**	**Distance 7.5 m**	**Distance 15 m**	**Distance 30 m**
Porous asphalt	Vitrumit	1.5 m	5.3/8.2	4.0/6.1	2.8/3.7
		4 m	2.5/1.9	3.8/2.9	3.6/3.1
Porous asphalt	Mineral wool and WWCB	1.5 m	7.8/9.6	7.0/7.8	6.2/5.9
		4 m	3.2/2.2	5.7/3.7	7.4/5
Lawn	Vitrumit	1.5 m	5.3/8.2	4.0/6.1	2.9/2.6
		4 m	2.5/1.9	3.8/2.9	3.7/3.1
Lawn	Mineral wool and WWCB	1.5 m	7.8/9.6	7.0/8.1	6.2/5.9
		4 m	3.2/2.2	5.7/3.7	7.4/5
-	Vitrumit	1.5 m	5.4/8.3	4.1/6.3	3.0/3.8
		4 m	2.5/1.9	3.9/3.0	3.6/3.3
-	Mineral wool and WWCB	1.5 m	8.2/9.8	7.5/8.1	6.7/6.2
		4 m	3.4/2.3	6.3/4.0	7.9/5.3
-	Hard screen	1.5 m	0.1/4.9	-1.8/1.7	-3.1/-1.5
		4 m	0.9/1.2	0.5/1.2	-1.7-0.3

Table 5.6: Insertion loss for Case 3.

The A-weighted SPL in 1/3 octave band are presented in the figure 5.7. The IL is displayed as the space between the reference curve and the curve of interest. In this section all three cases will be discussed simultaneously due to their similar behaviour. For all material and trench configurations, the IL starts around 63 Hz and varies depending of frequency. The highest IL occurs, for all configurations, around 160 Hz to 250 Hz as well as for high frequencies after 1 kHz. Consistent peaks at 1 kHz is observed for all configurations, resulting in a lower IL for all configurations. This peak could possibly occur due to constructive interference at 1 kHz.
It is clear that screen material mineral wool/WWCB results in higher IL, compared to Vitrumit, regardless of the use of trench-like segments, see Figure 5.7. It is also evident that the increased IL obtained from excluding the trench-like segments results from reduction of SPL for higher frequencies. When excluding trench-like segments, the IL is increased after 315 Hz for mineral wool/WWCB, and after 1 kHz for Vitrumit.

The results clearly shows that absorptive LHNS results in higher IL than non-absorbing LHNS (hard screens), see Figure 5.7. Absorbing LHNS performs better across the the entire frequency spectrum. It can also be noted that implementing hard screens might lead to increase SPL, evident for frequencies below 100 Hz and around the peak at 1 kHz.

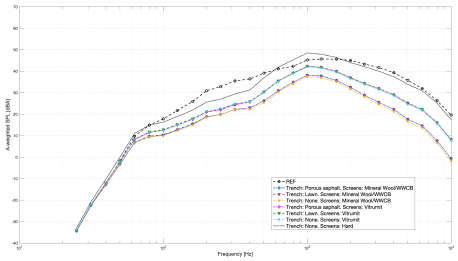

(a) Case 1

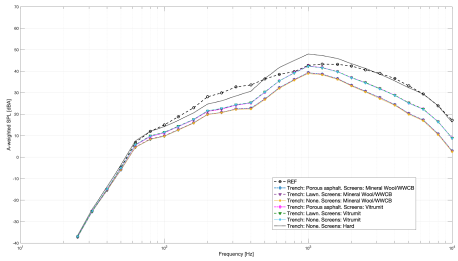

(b) Case 2

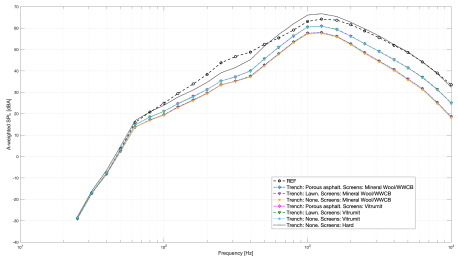

(c) Case 3

Figure 5.7: A-weighted SPL in 1/3-octave bands up to 10 kHz, comparing free-field conditions (no LHNS or trench-like segments) with various combinations of LHNS and trench-like segments at a distance of 15 meters from the source. Receiver height: 1.5 meters.

The A-weighted SPL in 1/3 octave band, for Cases 1, 2 and 3, at a receiver height of 1.5 meters and varying distances, is shown to illustrate the varying frequency content, see Figure 5.8, 5.9 and 5.10. For all three cases, it is evident that SoundPLAN shows similar insertion loss at both distances, indicating stable performance in the frequency range over distance.

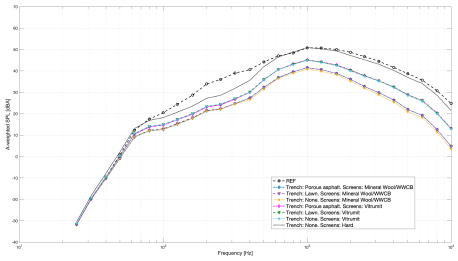

(a) Distance: 7.5 meters

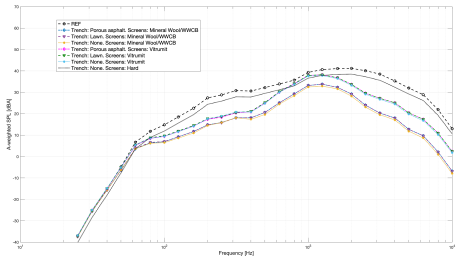

(b) Distance: 30 meters

Figure 5.8: A-weighted SPL for Case 1, without trench-like segments. Receiver height: 1.5 meters above ground.

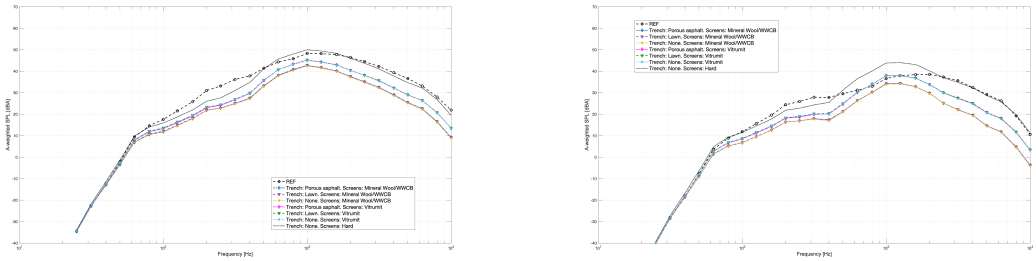

(a) Distance: 7.5 meters (b) Distance: 30 meters

Figure 5.9: A-weighted SPL for Case 2, without trench-like segments. Receiver height: 1.5 meters above ground.

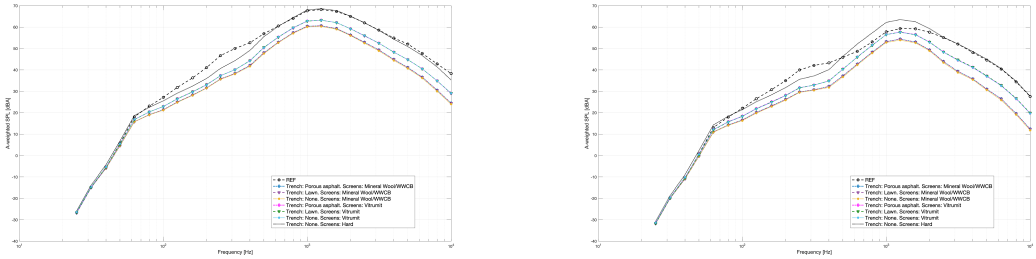

(a) Distance: 7.5 meters (b) Distance: 30 meters

Figure 5.10: A-weighted SPL for Case 3, without trench-like segments. Receiver height: 1.5 meters above ground.

5.2.2 Gibraltarvallen

The IL of the implemented real case scenario at Gibraltargatan is presented below. The IL is shown in Figure 5.11, calculated as the difference in facade noise levels with and without LHNS. For the two absorptive LHNS, a IL range of 5-8 dB is achieved on the ground floor of the facade facing the road. The IL decreases with increasing floor height, with floors two to five showing an IL of 2–4 dB, and the top two floors showing an IL of 0–1 dB. This effect could be because LHNS has a limited height, resulting in it being more effective shielding at lower heights. This is recurring for all results of Gibraltarvallen presented. A similar trend with decreasing IL over height can be observed on the south-east side of the studied building. For the IL_{Amax} at the road facing facade, shown in Figure 5.12, the IL ranges between 3-8 dB for floor one to three and drops to 0-1 dB for floor four to seven. Compared to the IL, IL_{Amax} decreases faster with floor height.

A comparison between implementing two or a single LHNS, shows an average IL_{Aeq} difference of 1 dB, see Figure 5.11. There is no difference in IL however for the two highest floors. Similar trends can be found for IL_{Amax}, see Figure 5.12.

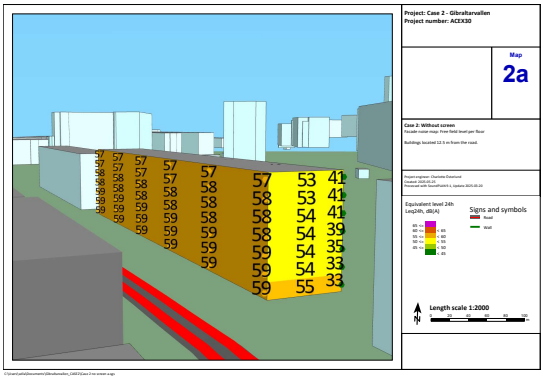

(a) Reference without LHNS

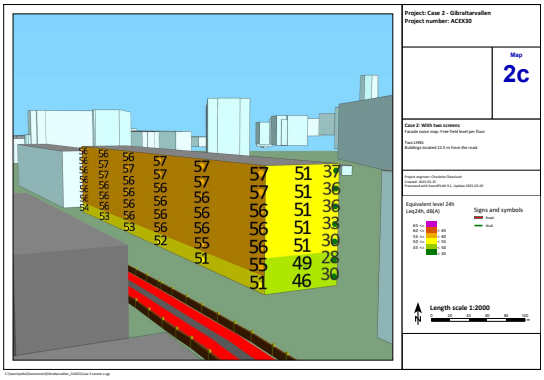

(b) Two absorptive LHNS

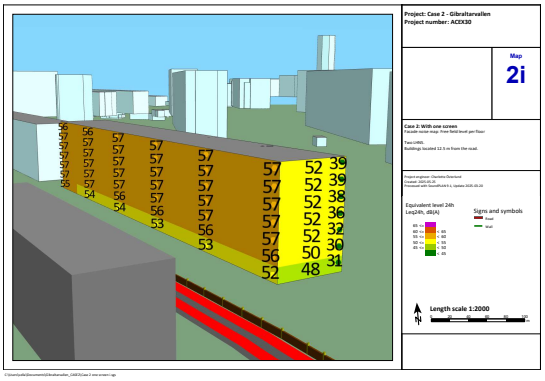

(c) One single absorptive LHNS

Figure 5.11: 3D model of Gibraltarvallen with a zoomed view of the facade closest to the road of the studied building. The building is coded by colours and numbers representing A-weighted equivalent continuous sound level over 24 hours ($L_{\mathrm{eq},24}$). The blue barriers represent LHNS and the red lines are the road (sound sources). Model reference case with one single absorptive LHNS and no trench-like segments.

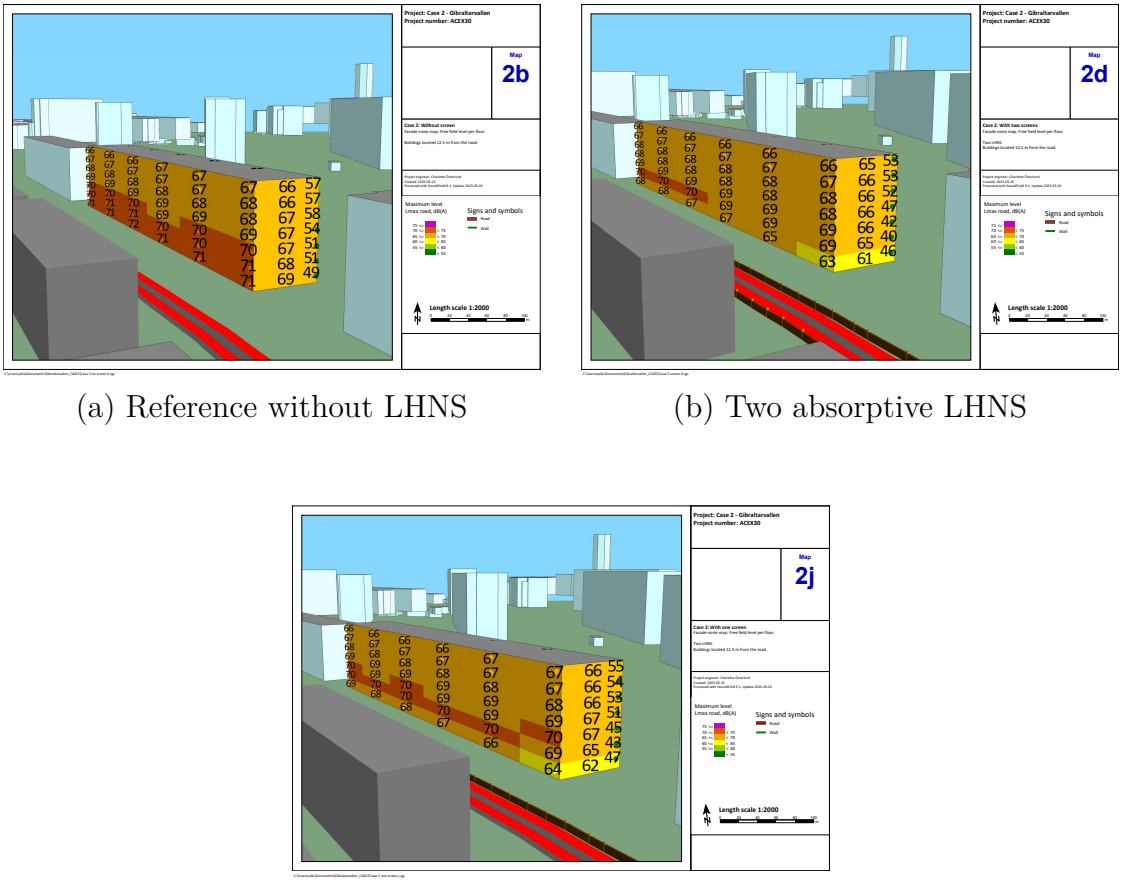

(a) Reference without LHNS

(b) Two absorptive LHNS

(c) One single absorptive LHNS

Figure 5.12: 3D model of Gibraltarvallen with a zoomed view of the facade closest to the road of the studied building. The building is coded by colours and numbers representing A-weighted maximum sound pressure level (Lmax) for road traffic noise. The blue barriers represent LHNS and the red lines are the road (sound sources). Model reference case with one single absorptive LHNS and no trench-like segments.

Figure 5.13 and 5.14 show grid maps of sound propagation for IL and L_{Amax}. The equivalent outdoor sound levels improves significant when placing LHNS along the road. In the area near the facade of the building, IL of up to 10 dB can be observed. Reductions are also visible on the sides of the building. The L_{Amax} changes significant in the area when LHNS are introduced. The peak noise levels for $\mathrm{IL}_{\mathrm{Amax}}$ are notably reduced.

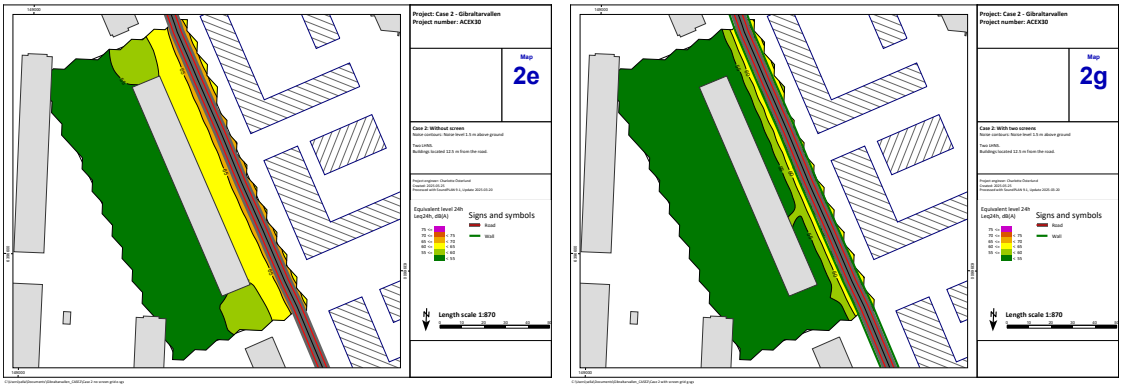

Figure 5.13: Grid maps of Gibraltarvallen with a zoomed view of the studied building. The area is coded by colours and numbers representing A-weighted equivalent continuous sound level over 24 hours ($L_{\mathrm{eq},24}$). Situation (1), reference without LHNS, is shown of the left, while situation (2), with LHNS, are displayed on the right.

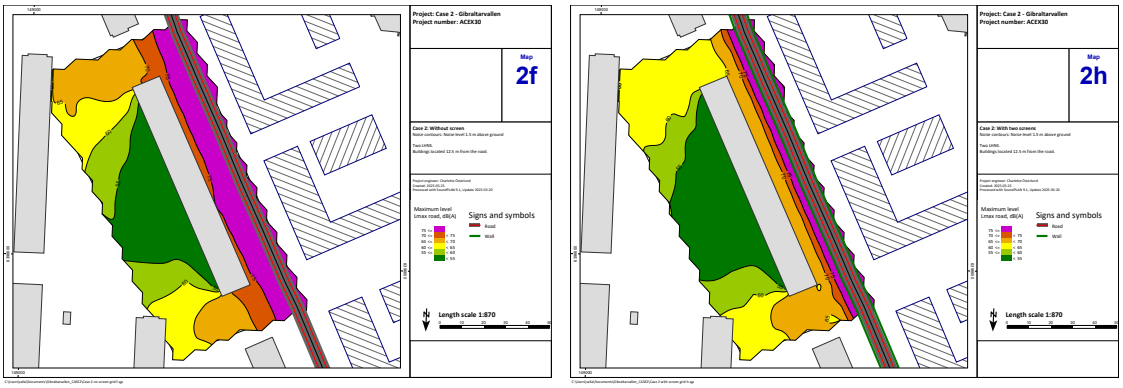

Figure 5.14: Grid maps of Gibraltarvallen with a zoomed view of the studied building. The area is coded by colours and numbers representing A-weighted maximum sound pressure level (L_{max}) for road traffic noise. Situation (1), reference without LHNS, is shown of the left, while situation (2), with LHNS, are displayed on the right.

5.3 Comparison between the methods

The results from BEM and SoundPLAN show tendencies of both similarities and differences. A similarity between the two methods is that the IL increases significantly when implementing absorptive LHNS compared to hard screens.

For both methods it is also evident that the insertion loss from using trench-like segments yield the exact same insertion loss regardless of the different materials tested. This indicates that, for both methods, it is better to remove it and get a closer distance between LHNS and road to increase IL. Both BEM and SoundPLAN show best IL results in all three cases when no trench is used in combination with mineral wool (type B (0.15/0.3) for BEM) or WWCB.

There are also differences between the results obtained from BEM and SoundPLAN. The IL achieved with BEM shows consistently higher results for all cases at the 1.5 meters receiver position. However, at the 7.5 and 15 meters for the 4

meters receiver position, SoundPLAN shows sometimes better IL results. One possible reason for that BEM predicts higher IL could be due to there is no modelled wind effects being considered in BEM. This can influence the sound propagation over longer distances. Comparing the IL results of mineral wool, the flow resistivity and the thickness matter in BEM, where smaller improvements were found when decreasing the flow resistivity. For the lower flow resistivity, increasing thickness also improved IL a bit more. In contrast, SoundPLAN treats the mineral wool and WWCB as a single material due to having the same absorption coefficient of 1. As a result, differences between mineral wool types cannot be evaluated.

Comparing the frequency spectra, minor differences in which frequency the IL begins can be observed. For BEM, IL begins around 63 HZ for Case 1 whereas, for Cases 2 and 3, the IL starts slightly later around 100 Hz. In contrast, SoundPLAN shows IL starting earlier than BEM, around 63 Hz for all three cases. Additionally, the frequency spectra show a peak at 80 Hz in all cases for BEM which is absent in the SoundPLAN results.

Comparing the real case scenario with Case 2 in BEM and simple simulation in SoundPLAN, show that on the ground floor at 1.5 meter receiver position, the IL for the real case is 5–8 dB compared to 11–12 dB for BEM and 7–8 dB for the simple simulation. For middle floor at around 4 meter receiver position, the IL for the real case is 2–4 dB compared to 4–8 dB for BEM and 3–6 dB simple calculation.

6
Discussion

6.1 The results

A key part of this investigation was the evaluation of trench-like segments, i.e. strips of soft ground. As the results show it was clear from both methods that trench-like segments did not prove to be beneficial in this acoustic context. The implementation of trench-like segments even resulted in a lowered IL, compared to without. This is most likely due to the placement of the absorptive low-height noise screens (LHNS), as the implementation of trench-like segments required moving the LHNS further away from the source. Since the screening is the most effective closest to the source, moving the absorbing LHNS reduced their effectiveness. Before this study was conducted, it was believed that introducing trench-like segments might compensate for this reduction, hopefully even perform better. This was however found not to be the case.

Both BEM and SoundPLAN with Nord2000 show that introducing a third absorptive LHNS between the driving lanes can increase the IL, although SoundPLAN suggests a stronger effect than BEM. Given the known limitations of SoundPLAN, its results might not be fully reliable. BEM, which is more robust in this context, confirms the trend but indicates a more modest improvement. Placing a barrier between the traffic lanes of a two-lane road could therefore have an acoustic impact, and Case 1 could be a concept to investigate further.

Introducing two absorptive LHNS seems to yield an insertion loss of 5-8 dB on the ground floor, with IL decreasing as facade height increases for the study case at Gibraltarvallen. However, compared to using a single LHNS, the average improvement at the facade level is about 1 dB. Such a small difference is unlikely to be perceptible to humans. Introducing two LHNS shows, compared to only one too small of a difference to be found a feasible solution. Multiple LHNS increases cost, maintenance and environmental impact that could not be justified with the acoustical impact. That said, when designing buildings and infrastructure, one must meet the Swedish regulations, and in some cases, a 1 dB improvement might be the difference between meeting or failing the legal requirements. From an acoustical standpoint, however, introducing two instead of a single LHNS would not be considered significant.

Mineral wool and WWCB perform significantly better than Vitrumit, especially at longer distances in SoundPLAN, where the difference in IL can reach several decibel. In BEM, however, the difference is less pronounced, with a maximum gain of 2 dB. Therefore, the choice of material could be based on other parameters than

acoustics, such a durability, substantiality and cost, since the acoustic performance of choosing mineral wool or WWCB instead of Vitrumit might not be justified. If one wants to apply mineral wool for LHNS, a trade-off between material types could be necessary. This depends on whether the priority is to invest in a mineral wool with higher flow resistivity, where thickness has little impact allowing for a thinner absorptive layer on the LHNS, or to use a material with lower flow resistivity, where increasing thickness leads to improved IL.

The results from BEM, for certain cases, show a peak at around 80 Hz, which may originate from the propulsion noise, i.e., engine. This highlights the challenge of the reducing low frequency components from propulsion vehicles. However, in today's cities an increasing share of electrical vehicles are used and is estimated to increase further in the future. The low-frequency components could therefore be expected to reduce due to the much weaker low-frequency components of electrical vehicles. Indicating that LHNS, which today struggle with addressing these frequencies, may become more effective in the future, in terms of their insertion loss in practice.

The results obtained from BEM and SoundPLAN indicate that absorptive LHNS could be another valuable tool in urban planning. These LHNS can be implemented in cities to reduce noise levels thereby contributing to a more sustainable and healthier urban environment. The findings also suggest that LHNS can be applied for different types of roads, making them suitable for implementation in a wide range of areas.

6.2 Difficulties and uncertainties

In BEM, the source placement was defined precisely with separate locations for propulsion and tyre/road noise along the x-z axis of the road. However, in SoundPLAN all sources are placed 1 meter from the centre of each lane. This leads to a simplified source model. The results show higher IL for BEM than for SoundPLAN, and one possible reason for this is the simplification in SoundPLAN. Additionally, when investigating absorptive LHNS it could be necessary to model the sources more accurately, as the simplified approach may not be sufficiently representative.

Further, SoundPLAN applies a default of -1 dB adjustment to account for reflective loss at facades. In some realistic cases, this loss could be less than 1 dB which can lead to an overestimation of attenuation. The adjustment is applied uniformly across all frequencies, which may not accurately reflect the real frequency dependence of reflection. It would have been preferable if this reflective loss could be frequency dependent, allowing for more precise modelling across different frequencies.

Both modelling approaches have limitations. The BEM simulations assume idealised conditions, such as flat ground and homogeneous materials. In BEM, wind effects are not considered which can influence the sound propagation and thereby affect the IL over distance. The BEM results show almost no decrease in IL over distance. This is probably due to this limitation. Reflections from nearby structures are also not included, which can significantly affect noise propagation in urban environments. In contrast, Nord2000 used in SoundPLAN, can possibly have light tailwind implemented, causing the IL to decrease more noticeable over distance compared to BEM.

As stated in Section 2.4, Nord2000 in SoundPLAN can in theory deal with multiple screens. However, in practice, it is typically implemented with a limitation of two diffracting barriers per sound path. Therefore, the results for Cases 1 and 3, which includes three LHNS, may have some uncertainties.

The maximum IL, i.e. the insertion loss for the maximum level, was also investigated using SoundPLAN but difficulties occurred when trying to obtain it from BEM and was unsuccessful. If the maximum IL could have been obtained for both methods, further comparison could have been made and potentially providing more insight.

6.3 Further work

The implementation of multiple absorbing LHNS in this thesis has only been studied through BEM and SoundPLAN simulations. It would be valuable to conduct field measurement to see whether using multiple absorbing LHNS actually work in practice. This would help validate the concept of multiple absorbing LHNS and at the same time show how well the result from SoundPLAN and BEM correspond with real measured data.

It would also be interesting to investigate how the increasing use of electric vehicles is expected to impact the performance of absorptive LHNS. How it will impact the results are partly unknown and will depend on how the characteristics of the vehicle change.

The absorptive LHNS studied in this thesis had a very traditional rectangular shape. Future studies could investigate if other shapes, such as angled or T-shaped screens, would increase the IL. It could also be worth testing additional materials that were not included here.

Lastly, future work could further investigate the feasibility of multiple absorptive LHNS. Even if the acoustic benefits are present, it might not always be worth implementing depending due to the cost, durability and maintenance.

7
Conclusion

The purpose of the thesis was to investigate the noise reduction potential of multiple absorptive low-height noise screens (LHNS) combined with trench-like road segments, i.e. strips of acoustically soft ground, in urban areas. Three cases of traffic road configurations were defined and evaluated for six types of absorbing materials for the LHNS and two variations of trench-like segments. To model the acoustic performance, two noise prediction tools, BEM and commercial noise mapping software SoundPLAN using the Nord2000 model, were used. Both methods evaluated the insertion loss (IL) at different heights (1.5 and 4 meters) and distances (7.5, 15 and 30 meters). A real-case scenario at Gibraltarvallen in Gothenburg was also simulated using SoundPLAN to assess practical applicability.

The results showed that absorptive LHNS, when placed close to the source and without trench-like segments, consistently improved insertion loss across all tested configurations. Both BEM and SoundPLAN confirmed significant reductions in A-weighted sound pressure levels, particularly at lower receiver heights. Simulations of the real-case scenario aligned well with the simplified models, supporting the general applicability of the findings.

Based on this and within the defined scope, the following questions could be answered:

- What levels of insertion loss (IL) can be achieved through absorptive low height noise screens in combination with trench-like segments, and are these reductions acoustically and perceptually significant?

  IL obtained from BEM and SoundPLAN varied depending on material, distance and receiver height. Highest IL was predicted at 1.5 meter height to 14.6 dB in BEM and 7.5 dB in SoundPLAN — both values considered perceptually and acoustically significant. As discussed above, the BEM results may overestimate the IL due to idealised conditions. For the higher receiver position at 4 meter, highest IL was 12.5 dB for BEM and 10.6 dB for SoundPLAN which are also significant. Trench-like segments were found to have no positive effect on IL. The implementation of trench-like segments showed a decreased IL compared to without trench-like segments, likely due to the increased distance between the absorptive LHNS and the sources.

- What is the most optimized design proposal tested from an acoustic perspective?

  It was found that the most optimized design proposal, according to both methods, excluded the trench-like segments and used mineral wool (type B for BEM)

or WWCB as the absorptive LHNS material. It was also shown that using an absorptive material on the LHNS improved the IL significantly across all cases. Additionally it was also found that excluding trench-like segments improved the IL in all cases.

- How well do our numerical calculations with BEM correspond to the simulations performed in SoundPLAN using the Nord2000 method? To what extent do these simulations reflect what would be expected in a real case scenario?

  The results obtained from BEM and SoundPLAN show that BEM consistently predicts higher IL values than SoundPLAN. This could be a result of BEM not accounting for wind effects, which may lead to higher predicted IL. When implementing Case 2 in a real case scenario at Gibraltarvallen (in SoundPLAN), IL was found to be 5–8 dB on the ground floor compared to 11–12 dB predicted by BEM. For the middle floors, SoundPLAN gave an IL of 2–4 dB compared to 4–8 dB predicted by BEM. It was found that numerical calculations in BEM predicts higher IL compared to the expected values from SoundPLAN calculations for a real-case based situation.

  When comparing the simple simulation of Case 2 in SoundPLAN with the geometry for Case 2 implemented in the real case scenario, a similar insertion loss was observed. For ground floor, the simple simulation showed an IL of 7–8 dB, and for middle floors 3–6 dB, which are similar to the results found in the real case application.

These results show that multiple absorptive LHNS offer a promising and effective noise reduction with potential of being implemented in urban planning. Their size and proven acoustic performance can make them suited for urban areas where traditional high barriers are undesirable or impractical.

The study also highlights that LHNS are particularly effective at reducing tyre/road noise rather than propulsion noise. As electric vehicles become more common, and traffic noise becomes increasingly dominated by tyre/road noise, LHNS may become even more relevant in future urban environments.

While the acoustic performance has been investigated under simulation conditions, further work is needed to validate the results through field measurements. It is also important to assess practical implementation aspects. Nonetheless, the findings provide a strong basis for considering multiple absorptive LHNS as a practical alternative to tall barriers in future urban planning.

The results show that the placement of the LHNS has a significant impact on the calculated IL. The improvement observed in IL when the trench-like segments were removed suggests that the position of the LHNS in relation to the sources is important. This highlights the importance of accurate source modelling if LHNS are to be considered in the future.

Bibliography

[1] M. Kleiner, *Acoustics and Audio Technology*. J.ROSS Publishing, 2012.

[2] C. Hoever and W. Kropp, "The boundary element method (bem) for radiation problems," Lecture notes, Chalmers University of Technology, https://www.ta.chalmers.se/content/protected/courses/ta2/LectureBEM_withNotes.pdf, 2017, accessed: February 20, 2025.

[3] H. G. Jonasson, "Acoustic source modelling of nordic road vehicles," SP Technical Research Institute of Sweden, Borås, Sweden, Tech. Rep. SP Report 2006:12, 2006. [Online]. Available: http://kunskapscentrumbuller.se/documents/Source%20modelling%20report%20final%20rev%20061017.pdf

[4] K. Larsson and H. Jonasson, "Uppdaterade beräkningsmodeller för vägtrafikbuller," SP Technical Research Institute of Sweden, Borås, Sweden, Tech. Rep. SP Report 2015:72, 2015.

[5] Folkhälsomyndigheten, "Buller," https://www.folkhalsomyndigheten.se/livsvillkor-levnadsvanor/miljohalsa-och-halsoskydd/halsoskydd/buller/, 2023, accessed: 2025-05-25. [Online]. Available: https://www.folkhalsomyndigheten.se/livsvillkor-levnadsvanor/miljohalsa-och-halsoskydd/halsoskydd/buller/

[6] C. Burgos and L. Wåssén, "A combination of a road restraint sys-tem and a noise reducing device," Master thesis, Chalmers University of Technology, Gothenburg, Sweden, 2017, [Online]. Available: https://hdl.handle.net/20.500.12380/253512.

[7] M. Hildén, "Modelling the effects of railway-implemented low-height noise screens," Master thesis, Chalmers University of Technology, Gothenburg, Sweden, 2024, [Online]. Available: http://hdl.handle.net/20.500.12380/307651.

[8] P. Eriksson, "Investigation of prediction methods for low height noise barrier implementation," Master thesis, Chalmers University of Technology, Gothenburg, Sweden, 2022, [Online]. Available: https://odr.chalmers.se/handle/20.500.12380/305800.

[9] B. van der Aa, "Road traffic noise reduction by multiple scattering and absorption mechanisms," Ph.D. dissertation, Chalmers University of Technology, Gothenburg, Sweden, 2015, DOI: 10.13140/RG.2.1.1112.3045.

[10] P. Jean, J. Defrance, and Y. Gabillet, "The importance of source type on the assessment of noise barriers," *Centre Scientifique et Technique du Bâtiment*, 1999.

[11] F. Fahy and D. Thompson, *Fundamentals of Sound and Vibration*, 2nd ed. CRC Press, 2015.

[12] H. Kuttruff, *Acustics - An introduction*. Taylor Francis, 2017.

[13] L. Beranek and T. Mellow, *Acoustics: Sound Fields and Transducers*. Elsevier, 2012.

[14] M. Möser, *Engineering Acoustics-An introduction to Noise Control*. Springer-Verlag Berlin Heidelberg, 2019.

[15] E. N. et al., "Grundläggande akustik," Lunds Tekniska Högskola, Teknisk Akustik, Tech. Rep. TVBA-3116, 2005.

[16] K. Attenborough, *Sound Propagation in the Atmosphere*. Springer, 2007.

[17] F. A. Everest and K. C. Pohlmann, *Master Handbook of Acoustics*, 7th ed. McGraw-Hill Education, 2020.

[18] G. Taraldsen, "The Delany-Bazley Impedance Model and Darcy's Law," *Acta Acustica united with Acustica*, 2005, norwegian University of Science and Technology.

[19] DELTA - Danish Electronics, Light & Acoustics, "Nord2000. Comprehensive Outdoor Sound Propagation Model. Part 1: Propagation in an Atmosphere without Significant Refraction." DELTA, Tech. Rep., 2001.

[20] K. Attenborough, I. Bashir, and S. Taherzadeh, "Outdoor ground impedance models," *Journal of the Acoustical Society of America*, vol. 129, no. 5, pp. 2806–2819, 2011.

[21] Y. Miki, "Acoustical proporties of porous materials -modifications of delany-bazley models-," *Journal of the Acoustical Society of Japan (E) 11, 1*, 1990.

[22] R. Kirby, "On the modification of delany and bazley formulae," *Applied Acoustics*, vol. 90, pp. 88–96, 2015, available online 12 June 2014.

[23] B. van der Aa and J. Forssén, "Time-domain simulations of low-height porous noise barriers with periodically spaced scattering inclusions," in *Forum Acusticum*. European Acoustics Association, 2014.

[24] Folkhälsomyndigheten, "Ljud och hälsa," Folkhälsomyndigheten, Tech. Rep. 18070-2, 2023.

[25] Nationell Samordning av buller, "Den nationella samordningen av omgivningsbuller rekommenderar beräkningsmetoden nord2000 vid utredning av buller från väg- och spårtrafik," 2024.

[26] H. G. Jonasson and S. Storeheier, "Nord 2000. new nordic prediction method for road traffic noise," SP Rapport 2001:10, Acoustics, Borås, Tech. Rep., 2001.

[27] J. Kragh, "Traffic noise prediction with nord2000 - an update," in *Proceedings of ACOUSTICS 2011*, 2011.

[28] J. Kragh, H. Jonasson, and B. P. et al., *User's Guide Nord2000 Road*, DELTA, SINTEF, SP, VTT, 2006.

[29] Göteborgs Stad. (2025) 3da utrymme fordonstrafik. Göteborgs Stad. Kapitel i Teknisk Handbok. Läst 2025-05-06. [Online]. Available: https://tekniskhandbok.goteborg.se/3-utformning/3d-fordonstrafik/3da-utrymme-fordonstrafik/

[30] Trafikverket, "KRAV TRVINFRA-00396: Vägutformning - Vägars och gators utformning," Trafikverket, Tech. Rep. TRVINFRA-00396, 2024, published 2024-11-01.

[31] ——, "Krav grundvärden: Vägars och gators utformning," Trafikverket, Tech. Rep. 2024:148, 2024, published 2024-11-01.

[32] D. Duhamel, "Efficient calculation of the three-dimensional sound pressure field around a noise barrier," *Journal of Sound and Vibration*, vol. 197, no. 5, pp. 547–571, 1996, received 4 November 1993, and in final form 25 March 1996.

[33] M. Baulac, J. Defrance, P. Jean, and F. Minard, "Efficiency of noise protections in urban areas: Predictions and scale model measurements," *Acta Acustica united with Acustica*, vol. 92, pp. 530–539, 2001.

[34] Boverket, "Frågor och svar om buller," 2016, promemoria, publicerad 2016-06-01. [Online]. Available: https://www.boverket.se/sv/PBL-kunskapsbanken/teman/buller/fragor-och-svar-om-buller/

[35] M. Waaranperä, "Acoustic effect of sound absorbing materials and surfaces in road infrastructure," Licentiate thesis, Chalmers University of Technology, Sweden, 2024.

[36] B. Botterman, "Wwcb characterizing, modelling and optimizing the sound absorption of wood wool cement boards," Master thesis, Eindhoven University of Technology, 2016. [Online]. Available: https://research.tue.nl/en/studentTheses/844af00f-f77f-470d-b255-8d273fb489c1

[37] C. Liu, F. Georgiou, and M. Hornikx, "Characterisation of the acoustic impedance of vegetated roofs with a multiple-geometry approach," *Applied Acoustics*, vol. 199, 2022.

A

Appendix 1

Frequency	Tyre/road noise						Propulsion noise					
	Cat. 1		Cat. 2		Cat. 3		Cat. 1		Cat. 2		Cat. 3	
	a_R	b_R	a_R	b_R	a_R	b_R	a_P	b_P	a_P	b_P	a_P	b_P
25	69.9	33	86.8	2	76.5	33.0	94.0	0	79.5	33	94.7	0
31.5	69.9	33	88.6	2	76.5	33.0	94.7	0	99.5	33	94.3	0
40	69.9	33.0	88.5	0.0	76.5	33.0	95.5	0.0	79.5	33.0	95.2	0.0
50	74.9	30.0	89.5	0.0	78.5	30.0	95.5	0.0	81.5	30.0	100.3	0.0
63	74.9	30.0	93.6	2.0	79.5	30.0	98.5	0.0	82.5	30.0	104.9	0.0
80	74.9	30.0	91.2	2.0	79.5	30.0	98.4	0.0	82.5	30.0	102.4	0.0
100	79.3	41.0	89.0	4.0	82.5	41.0	94.0	0.0	85.5	41.0	98.0	0.0
125	82.5	41.2	84.4	2.0	84.3	41.2	93.5	0.0	87.3	41.2	98.0	0.0
160	81.3	42.3	83.1	2.0	84.3	42.3	92.2	0.0	87.3	42.3	98.3	0.0
200	80.9	41.8	83.1	6.0	84.3	41.8	96.6	0.0	87.3	41.8	98.3	0.0
250	79.9	38.6	84.2	8.2	88.4	38.6	97.7	8.5	91.4	38.6	99.5	8.5
315	79.8	35.5	83.5	8.2	89.2	35.5	98.0	8.5	92.2	35.5	100.0	8.5
400	81.5	31.7	82.6	8.2	93.0	31.7	95.3	8.5	96.0	31.7	99.0	8.5
500	88.0	25.9	77.6	8.2	95.1	25.9	91.2	8.5	98.1	25.9	98.4	8.5
630	89.7	26.5	77.7	8.2	97.5	26.5	89.4	8.5	100.5	26.5	96.4	8.5
800	91.8	32.5	75.8	8.2	97.8	32.5	90.4	12.5	100.8	32.5	92.1	8.5
1000	94.3	37.7	76.3	8.2	96.6	37.7	92.5	12.5	99.6	37.7	92.8	8.5
1250	93.5	41.4	79.4	8.2	94.0	41.4	93.0	12.5	97.0	41.4	92.3	8.5
1600	91.8	41.6	80.7	8.2	92.9	41.6	90.8	12.5	95.9	41.6	89.2	8.5
2000	88.4	42.3	80.4	9.5	89.5	42.3	90.4	12.5	92.5	42.3	90.2	8.5
2500	85.4	38.9	78.3	9.5	85.1	38.9	89.1	12.5	88.1	38.9	87.7	8.5
3150	81.6	39.5	78.8	9.5	82.1	39.5	87.1	12.5	85.1	39.5	85.8	8.5
4000	77.7	39.6	76.9	9.5	79.2	39.6	84.9	12.5	82.2	39.6	84.5	8.5
5000	75.7	39.8	74.9	9.5	76.3	39.8	82.6	12.5	79.3	39.8	82.9	8.5
6300	72.6	40.2	72.1	9.5	74.3	40.2	82.7	8.5	77.3	40.2	83.9	8.5
8000	70.0	40.8	70.1	9.5	75.3	40.8	79.6	8.5	78.3	40.8	80.8	8.5
10000	68.5	41.0	66.5	9.5	78.3	41.0	76.5	8.5	81.3	41.0	77.3	8.5

Table A.1: Sound power coefficients, Nord2005 [3].

Table A.2: Correction values for $a_R[4]$.

f	250	315	400	500	630	800	1k	1,25k	1,6k
	1	1	1	1	1	1	1	1	-1

f	2k	2,5k	3,15k	4k	5k	6,3k	8k	10k
	-2	-3	-4	-5	-4	-3	-2	1

Table A.3: Correction values for $a_P[4]$.

f	25	31,5	40	50	63	80	100	125	160	250	315	400
	-3	-3	-3	-3	-3	-3	-3	-3	-3	-3	-3	-3

f	500	630	800	1k	1,25k	1,6k	2k	2,5k	3,15k	4k	5k	6,3k
	-3	-3	-3	-3	-3	-3	-3	-3	-3	-3	-3	-3

B

Appendix 2

Table B.1: A-weighting coefficients for third-octave centre frequencies

Frequency (Hz)	**A-weighting Coefficient (dB)**
25	-44.7
31.5	-39.4
40	-34.6
50	-30.2
63	-26.2
80	-22.5
100	-19.1
125	-16.1
160	-13.4
200	-10.9
250	-8.6
315	-6.6
400	-4.8
500	-3.2
630	-1.9
800	-0.8
1000	0
1250	0.6
1600	1.0
2000	1.2
2500	1.3
3150	1.2
4000	1.0
5000	0.5

DEPARTMENT OF ARCHITECTURE AND CIVIL ENGINEERING, DIVISION OF APPLIED ACOUSTICS
CHALMERS UNIVERSITY OF TECHNOLOGY
Gothenburg, Sweden
www.chalmers.se